Preprints.org

Article

Not peer-reviewed version

Global Food Price Dynamics, Undernourishment and Human Development: Wavelet Coherence Evidence and SDG 2.1 Resilience Scenarios to 2030

Olena Pavlova *, Oksana Liashenko *, Kostiantyn Pavlov *, Agata Kutyba, Nataliia Fastovets, Artur Machno, Oleksandr Holubiev, Tetiana Vlasenko

Posted Date: 11 March 2026

doi: 10.20944/preprints202603.0754.v1

Keywords: food price volatility; undernourishment; SDG 2; wavelet coherence; food security; human development; scenario analysis; sustainable development

Preprints.org is a free multidisciplinary platform providing preprint service that is dedicated to making early versions of research outputs permanently available and citable. Preprints posted at Preprints.org appear in Web of Science, Crossref, Google Scholar, Scilit, Europe PMC.

Copyright: This open access article is published under a Creative Commons CC BY 4.0 license, which permit the free download, distribution, and reuse, provided that the author and preprint are cited in any reuse.

Preprints.org (www.preprints.org) | NOT PEER-REVIEWED | Posted: 11 March 2026 doi:10.20944/preprints202603.0754.v1

Disclaimer/Publisher's Note: The statements, opinions, and data contained in all publications are solely those of the individual author(s) and contributor(s) and not of MDPI and/or the editor(s). MDPI and/or the editor(s) disclaim responsibility for any injury to people or property resulting from any ideas, methods, instructions, or products referred to in the content.

Article

Global Food Price Dynamics, Undernourishment and Human Development: Wavelet Coherence Evidence and SDG 2.1 Resilience Scenarios to 2030

Olena Pavlova [1,2,*], Oksana Liashenko [2,3,*], Kostiantyn Pavlov [2,*], Agata Kutyba [1], Nataliia Fastovets [4], Artur Machno [1], Oleksandr Holubiev [5] and Tetiana Vlasenko [6,7]

[1] Faculty of Management, AGH University of Krakow, Al. Mickiewicz 30, 30-059 Kraków, Poland
[2] Faculty of Economics and Management, Lesya Ukrainka Volyn National University, Voli Ave., 13, 43-025 Lutsk, Volyn Oblast, Ukraine
[3] Loughborough Business School, Loughborough University, Epinal Way, Loughborough LE11 3TU, UK
[4] Faculty of Economics and Management, Kyiv National University of Technologies and Design., 2 Mala Shyianovska St., 2, Kyiv, 01011, Ukraine
[5] Department of Enterprise Economics and Management, Academy of Labour, Social Relations and Tourism, Kiltseva Road, 3-A, Kyiv, 08131 Ukraine
[6] Academy of Silesia, ul. Rolna 43, 40-555, Katowice, Poland
[7] Business and Administration Department, Simon Kuznets Kharkiv National University of Economics, Nauky Ave., 9-A, 61165, Kharkiv, Ukraine
* Correspondence: pavlovkostya@gmail.com (K.P.); o.liashenko@lboro.ac.uk (O.L.); strishenez@gmail.com (O.P.); tel.: +380972830808 (KP)

Abstract

This study examines whether international food price dynamics provide a reliable signal of undernourishment and human development outcomes relevant to the attainment of SDG 2 (Zero Hunger) by 2030. We apply wavelet coherence analysis to the FAO Food Price Index and the prevalence of undernourishment (SDG Indicator 2.1.1) over 2001–2023, testing statistical significance against an AR(1) red-noise null hypothesis. Hybrid ARIMA–Random Forest models generate probabilistic price forecasts through 2030. Despite strong raw coherence ($R^2 \approx 0.77$), only 7.8% of time–frequency cells achieve statistical significance, indicating that apparent co-movement largely reflects autocorrelation rather than substantive dependence. Where significant coherence emerges, it concentrates at medium-run horizons (3–6 years), consistent with undernourishment as a habitual dietary adequacy measure linked to sustained affordability pressures affecting health, productivity, and human capital formation. Rolling correlation analysis reveals a regime shift around 2012—from negative to positive correlation—coinciding with a slowdown in progress toward reducing hunger. Price forecasts exhibit rapidly widening confidence intervals (by ±131 index points by 2030), underscoring fundamental limits to predictability. These findings caution against mechanistic inferences from global price indices to hunger and human development outcomes, redirecting policy emphasis toward domestic transmission channels and nutrition-sensitive safety nets.

Keywords: food price volatility; undernourishment; SDG 2; wavelet coherence; food security; human development; scenario analysis; sustainable development

1. Introduction

Achieving Sustainable Development Goal 2 (SDG 2: Zero Hunger) is central to sustainable development because food insecurity and undernutrition directly undermine health, learning, labour productivity, and social stability, while also reinforcing poverty traps and widening inequalities. In the United Nations SDG framework, Target 2.1 commits countries to ensuring access to safe,

© 2026 by the author(s). Distributed under a Creative Commons CC BY license.

Preprints.org (www.preprints.org) | NOT PEER-REVIEWED | Posted: 11 March 2026 doi:10.20944/preprints202603.0754.v1

nutritious, and sufficient food for all people year-round by 2030 [1]. Yet recent global monitoring emphasises that progress is fragile and increasingly exposed to overlapping shocks, including macroeconomic disruptions, climate extremes and conflict-related disturbances that destabilise food systems and household purchasing power. These interconnected pressures heighten the need for empirical tools that can distinguish transient stress signals from persistent, policy-relevant risks to human development.

A widely used global stress indicator is the FAO Food Price Index (FPI), which tracks monthly international prices across major commodity groups. Because many countries depend on food imports for dietary staples and because traded commodity prices shape domestic price formation through exchange rates, market integration and policy responses, global price movements are often treated—implicitly or explicitly—as a proxy for hunger risk. Policy reporting, therefore, frequently juxtaposes food price dynamics with food security concerns, including in the World Bank's periodic assessments of commodity markets and food security conditions [2–4]. However, treating international prices as a direct measure of hunger risk can be analytically problematic: price shocks do not transmit uniformly across countries, and the welfare incidence depends on domestic pass-through, wage dynamics, social protection coverage and the structure of food systems [5,6].

A second challenge concerns the outcome measure used for SDG accountability. The prevalence of undernourishment (PoU)—SDG Indicator 2.1.1—measures the share of the population whose habitual dietary energy intake falls below minimum requirements, estimated using a probabilistic model and reported annually [7]. PoU is therefore well-suited to tracking structural progress in nutrition-related human development, but it is not designed to respond mechanically to short-lived monthly price volatility. As a result, simple global correlations between an international monthly price index and annual undernourishment may reflect shared slow-moving components (persistence and trends) rather than a stable, policy-actionable relationship.

Existing research provides strong conceptual and empirical reasons to expect that food prices matter for food security, while also highlighting that the relationship may be heterogeneous, state-dependent, and time-varying. Studies of food price spikes and commodity-market behaviour emphasise that surges can arise from interacting drivers—stocks, energy linkages, weather variability, and policy responses—rather than from a single disturbance, and that volatility can persist when policy responses amplify uncertainty [5,6]. Policy-oriented work similarly documents the trade-offs governments face during price spikes, where interventions may stabilise domestic markets but generate distortions and spillovers if implemented in an uncoordinated or ad hoc manner [9]. At the same time, sustainability-relevant impacts operate through multiple transmission channels: real-income compression and poverty exposure (SDG 1), diet quality and health consequences (SDG 3 and SDG 2.2), and the way climate and conflict shocks jointly affect prices and vulnerability. The implication is that the "food price–hunger" nexus is unlikely to be well captured by a constant-parameter, full-sample correlation.

This paper addresses these issues by reframing the empirical question. Rather than seeking a single global elasticity of undernourishment with respect to international prices—an exercise complicated by endogeneity and by the joint influence of income growth, exchange rates, conflict, climate and policy—we ask: when, and at which horizons, do international food prices and undernourishment co-move in a statistically defensible way? This is a sustainability-relevant question because SDG planning requires identifying whether price dynamics provide a meaningful risk signal for hunger outcomes, and whether that signal is concentrated in short-run volatility episodes or in longer-run affordability pressures that erode resilience.

Methodologically, we use time–frequency (wavelet) analysis to accommodate non-stationarity, crisis regimes and structural change. Wavelet power describes how variance evolves across time and scales, while wavelet coherence measures localised dependence between two series in time–frequency space [10]. A crucial feature of our design is that coherence is assessed against an autocorrelated red-noise benchmark, consistent with the methodological warning that persistent series can exhibit visually strong coherence even under independence. This benchmarking is not a

© 2026 by the author(s). Distributed under a Creative Commons CC BY license.

Preprints.org (www.preprints.org) | NOT PEER-REVIEWED | Posted: 11 March 2026 doi:10.20944/preprints202603.0754.v1

technical footnote; it is a safeguard against drawing inferences about sustainability and SDGs from dependence patterns that may be largely driven by autocorrelation rather than substantive co-movement [10,11].

In addition, we connect diagnostics to forward-looking SDG planning through scenario-oriented projections to 2030. Global commodity prices are difficult to forecast at multi-year horizons because the drivers of tail events—geopolitical disruptions, extreme weather and policy breaks—are inherently uncertain [3,6]. Accordingly, we interpret projections as scenario-based stress tests rather than deterministic forecasts: the objective is to quantify exposure under plausible baseline and adverse price paths, recognising that non-price drivers (income trajectories, safety nets, fragility and climate risks) remain decisive for undernourishment outcomes [2,3,7].

The paper makes three contributions. First, it provides a statistically disciplined reassessment of the global co-movement between international food prices and undernourishment, explicitly separating visually compelling dependence from dependence that remains significant after accounting for persistence. Second, it highlights regime dependence and structural change, aligning the empirical strategy with the reality of food-system sustainability under shifting macro-climate-conflict conditions rather than stable equilibria. Third, it translates uncertainty into SDG-relevant planning evidence by using scenario logic to inform anticipatory governance and resilience policy, emphasising transmission channels (domestic pass-through, purchasing power protection, and nutrition-sensitive safety nets) rather than relying on global price indices as a sufficient proxy for hunger.

The remainder of the paper proceeds as follows. Section 2 reviews the literature on food price dynamics, transmission mechanisms and time–frequency approaches. Section 3 describes the data, including the construction and interpretation of the FPI and PoU. Section 4 outlines the empirical strategy, including wavelet power, coherence with red-noise benchmarking, and the forecasting and scenario framework. Section 5 presents results. Section 6 discusses implications for sustainable development policy and human development outcomes. Section 7 concludes.

2. Literature Review

2.1. Food Price Volatility, Food Security, and Human Development: Conceptual Linkages

The ambition to "end hunger and ensure access by all people… to safe, nutritious and sufficient food all year round" by 2030 (SDG Target 2.1) places renewed analytical emphasis on the macro-micro linkages through which food price dynamics translate into food insecurity, undernourishment, and ultimately constrained human development [1]. Food security exists when "all people, at all times have physical and economic access to sufficient, safe and nutritious food that meets their dietary needs and food preferences for an active and healthy life" [7]. This definition underscores that food insecurity negatively affects human physical, social, emotional, and cognitive development throughout the life course [12]. The relationship among food security, nutrition, and human development forms a triangular linkage: empirical studies consistently demonstrate a strong negative correlation between the human development index (HDI) and food insecurity—countries with high food insecurity tend to have lower human development outcomes, and vice versa [13].

This link has become more salient since the mid-2010s, as progress in reducing hunger has stalled and, in many contexts, reversed amid overlapping shocks. Recent global assessments underscore that conflict, economic disruptions, and climate extremes increasingly interact to destabilise food systems, undermine purchasing power, and erode diet quality—mechanisms central not only to SDG 2 (Zero Hunger) but also to SDG 1 (No Poverty), SDG 3 (Good Health and Well-being), and broader human development outcomes [14–19]. The 2025 Global Hunger Index emphasises that political commitment at the highest levels is needed to prevent famine, as millions face violations of their human right to adequate food [20].

We invoke these SDG linkages not as a broad descriptive catalogue, but because they map onto distinct transmission channels affecting human development. SDG 1 captures the real-income and

© 2026 by the author(s). Distributed under a Creative Commons CC BY license.

Preprints.org (www.preprints.org) | NOT PEER-REVIEWED | Posted: 11 March 2026 doi:10.20944/preprints202603.0754.v1

poverty pathway through which food inflation constrains access; SDG 3 and Target 2.2 capture nutrition-related consequences via diet quality and child undernutrition—critical determinants of human capital formation; SDG 13 and SDG 16 reflect climate- and conflict-related shocks that can both trigger price surges and magnify their welfare incidence. This channel-based framing motivates a time-varying empirical strategy rather than a constant-parameter representation.

2.2. Global Food Price Dynamics: Drivers, Episodes, and Structural Complexity

A substantial body of literature documents pronounced volatility and episodic spikes in international food prices, driven by supply shocks, demand shifts, energy-fertiliser pass-through, policy interventions, macroeconomic conditions, and market expectations. The 2007–2008 and 2010–2011 crises prompted extensive work on how biofuel mandates, inventory dynamics, trade restrictions, and commodity financialisation can amplify short-run price pressures [5,21,22]. Subsequent episodes—particularly the 2021–2023 period—have been characterised by "compound shocks," including pandemic-related supply chain disruptions, conflict-related export constraints, energy price surges affecting input costs, and shifts in global monetary conditions [2].

The State of Food Security and Nutrition in the World 2024 reports that global food price inflation peaked at 13.6 per cent in January 2023, significantly outpacing headline inflation by 5.1 percentage points. Low-income countries experienced even steeper increases, with annual food inflation rates peaking at over 50 per cent in August 2024 [18]. A 10 per cent increase in domestic food prices is associated with a 3.5 per cent rise in the number of people suffering food insecurity, with particularly severe impacts in countries with high income disparities [18]. This complexity is also evident in the growing emphasis on the affordability of healthy diets in global monitoring: the average cost of a healthy diet rose to 4.46 purchasing power parity dollars per person per day in 2024, leaving approximately 2.60 billion people unable to afford such diets [18].

2.3. Transmission from Prices to Food Security, Nutrition, and Human Development

The welfare consequences of higher food prices are theoretically ambiguous at the aggregate level because they redistribute income between net food consumers and net food producers; nonetheless, empirical evidence repeatedly shows that, in many low-income settings, net consumer effects dominate and poverty rises when staple prices surge [23]. Price increases can reduce real incomes, induce substitution toward cheaper calorie sources, and diminish dietary diversity—mechanisms consistent with nutritional deterioration even when caloric intake declines less sharply. These effects have profound implications for human development, particularly child cognitive development, educational outcomes, and long-term productivity [24].

In a large multi-country analysis, Headey and Ruel [25] document a significant association between food inflation and child undernutrition in low- and middle-income countries, highlighting the sensitivity of nutritional outcomes to price environments beyond household-level shocks. Their findings demonstrate that food price inflation is associated with increased child wasting and stunting—key indicators for both SDG Target 2.2 and the human development dimension of health and longevity. The interplay between prices and fragility is particularly important for SDG-relevant trajectories. Contemporary crisis reporting shows that acute food insecurity is increasingly concentrated in conflict-affected and climate-exposed contexts, where coping capacity is low, and market disruptions are severe [19].

At the same time, public policy responses to price surges—such as export bans, price controls, consumer subsidies, and buffer stock operations—can dampen domestic price volatility while introducing distortions or shifting burdens abroad. Pieters and Swinnen [9] formalise the trade-off between stabilisation and distortions when governments intervene under constrained policy sets. This trade-off is SDG-relevant: stabilisation measures may protect poor consumers in the short run (supporting SDG 2.1 and SDG 1), yet may undermine incentives for production and long-run resilience.

© 2026 by the author(s). Distributed under a Creative Commons CC BY license.

Preprints.org (www.preprints.org) | NOT PEER-REVIEWED | Posted: 11 March 2026 doi:10.20944/preprints202603.0754.v1

2.4. Empirical Challenges and Methodological Approaches

Empirically identifying a robust price-hunger relationship is challenging for three reasons. First, both price indices and hunger indicators commonly display persistence, structural breaks, and non-linear dynamics, making inference sensitive to model specification. Second, relationships are plausibly time-varying: prices may matter most during crises, when liquidity constraints bind, and substitution possibilities narrow, but appear weaker in "normal times." Third, conventional time-domain approaches may obscure the possibility that co-movement differs across horizons [26].

These concerns have stimulated interest in frequency-domain and time-frequency methods. Wavelet analysis has become a standard approach for decomposing non-stationary time series into localised time-frequency representations [10]. Its appeal in macro-financial and commodity settings stems from its ability to capture transient co-movements, regime shifts, and multi-scale dynamics within a unified framework. Applications to commodity markets demonstrate how wavelets reveal horizon-specific integration and evolving co-movement strengths over time [27,28].

For food security research, wavelet coherence extends wavelet power analysis by estimating the local correlation structure between two series across time and frequency bands. The methodological foundations are well established: Torrence and Compo [10] provide core guidance on continuous wavelet transforms and inference issues, while Grinsted et al. [11] formalise the cross-wavelet transform and wavelet coherence with Monte Carlo significance testing against red-noise nulls. Maraun and Kurths [29] further address the pitfalls of significance testing, cautioning against spurious coherence findings—a particularly important consideration when analysing highly autocorrelated series such as food prices and hunger indicators.

2.5. Forecasting Food Prices and SDG-Relevant Scenario Analysis

A parallel literature addresses the forecasting of commodity and food prices using both econometric and machine learning methods. Traditional time-series models (e.g., ARIMA variants) can capture persistence and seasonality [30,31], whereas nonlinear methods, such as Long Short-Term Memory (LSTM) networks, can capture interactions and regime-dependent responses when sufficient data are available [32,33]. Recent practice increasingly favours hybrid strategies that combine the strengths of linear stochastic structure and flexible non-linear correction, particularly for series with both trend and episodic turbulence. Paul et al. [34] demonstrate that random forest-based ARIMA-LSTM hybrid models can improve forecasting accuracy by 8-25% for volatile agricultural price series compared to conventional statistical models.

In the context of SDG policy, forecasting becomes relevant to the extent that it enables scenario analysis and risk quantification for 2030 commitments. International monitoring bodies increasingly emphasise uncertainty ranges rather than point estimates, both for hunger indicators and for price outlooks. SOFI 2025 focuses on representing uncertainty in global hunger figures and on the role of food price inflation in shaping affordability [18]. Meanwhile, the World Bank's Commodity Markets Outlook provides forward-looking assessments of commodity price trajectories under macroeconomic uncertainty, complementing early warning narratives that highlight the interactions among policy uncertainty, trade disruptions, and climate variability [2].

2.6. Research Gap and Contribution

Synthesising these strands reveals clear research gaps. First, while the qualitative link between food prices, food security, and human development is widely recognised, empirical evidence on when and at which horizons food price movements co-move with SDG-relevant hunger indicators remains uneven. Second, much of the policy discussion implicitly assumes a stable relationship, even though theory and crisis experience indicate state dependence and multi-scale dynamics. Third, forecasting exercises often remain disconnected from explicit assessments of SDG targets, limiting their usefulness for planning and accountability. Fourth, the human development dimension—

© 2026 by the author(s). Distributed under a Creative Commons CC BY license.

Preprints.org (www.preprints.org) | NOT PEER-REVIEWED | Posted: 11 March 2026 doi:10.20944/preprints202603.0754.v1

particularly the pathway from food prices through nutrition to cognitive and physical development outcomes—requires more explicit analytical treatment.

The present study directly addresses these limitations by (i) using wavelet power and coherence to characterise time-frequency structure and statistically significant co-movement under red-noise nulls [10,11], (ii) interpreting horizon-specific phase relationships in light of crisis mechanisms and policy responses, (iii) integrating forecast uncertainty into scenario-based projections of SDG 2.1 attainment risks, and (iv) framing findings within the broader human development context consistent with the interconnected SDG framework. In doing so, the study aligns econometric design with the practical requirements of SDG governance: identifying which price horizons matter most for hunger outcomes and human development, distinguishing robust signals from spurious co-movement, and translating statistical uncertainty into policy-relevant scenario narratives.

In this section, where applicable, authors are required to disclose details of how generative artificial intelligence (GenAI) has been used in this paper (e.g., to generate text, data, or graphics, or to assist in study design, data collection, analysis, or interpretation). The use of GenAI for superficial text editing (e.g., grammar, spelling, punctuation, and formatting) does not need to be declared.

3. Data

3.1. Data Sources and Sample Construction

This study employs a comprehensive dataset combining international food price indices with global hunger indicators to examine the time-frequency dynamics of food price transmission to food security outcomes. Our primary data sources include the Food and Agriculture Organisation of the United Nations (FAO) and the World Bank, both of which maintain rigorously validated statistical databases with extensive temporal coverage.

FAO Food Price Index (FPI). The FAO Food Price Index is a measure of the monthly change in international prices of a basket of food commodities. It is the average of five commodity group price indices, weighted by the average export shares of each group for the 2014-2016 reference period [14]. Monthly data are available from January 1990. For long-run spectral analysis, we additionally compiled annual indices extending back to 1961, enabling examination of multi-decadal price dynamics encompassing multiple food price crises. The index is rebased to 2014-2016 = 100.

Prevalence of Undernourishment (PoU). As the official SDG Indicator 2.1.1, the PoU measures the proportion of the population whose habitual food consumption is insufficient to provide the dietary energy levels required to maintain a normal, active and healthy life [17]. This indicator, curated by FAO as the custodian UN agency, is derived from country data on food supply, food consumption, and energy needs, and incorporates demographic characteristics such as age, sex, and physical activity levels. Country-level and global aggregate data are available from 2001.

Supplementary indicators. To enable robustness checks and heterogeneity analysis, we also collected data on food import dependence (food imports as a percentage of merchandise imports), GDP per capita, and regional classifications from the World Bank's World Development Indicators database.

3.2. Variable Definitions and Measurement

Table 1 provides detailed definitions and descriptive statistics for all variables employed in the analysis.

Table 1. Variable Definitions and Descriptive Statistics.

Variable	Definition	Period	Mean	Std. Dev.
FPI	FAO Food Price Index (2014-2016=100)	1990M1-2025M12	99.7	24.3
FPI_Cereals	FAO Cereals Price Index	1990M1-2025M12	102.4	28.6
FPI_Oils	FAO Vegetable Oils Price Index	1990M1-2025M12	105.8	35.2
FPI_Meat	FAO Meat Price Index	1990M1-2025M12	98.5	18.7

© 2026 by the author(s). Distributed under a Creative Commons CC BY license.

Preprints.org (www.preprints.org) | NOT PEER-REVIEWED | Posted: 11 March 2026 doi:10.20944/preprints202603.0754.v1

FPI_Dairy	FAO Dairy Price Index	1990M1-2025M12	101.2	29.4
FPI_Sugar	FAO Sugar Price Index	1990M1-2025M12	97.3	32.8
PoU_Global	Global prevalence of undernourishment (%)	2001-2023	9.8	1.9
FPI_Annual	Annual FAO Food Price Index	1961-2025	72.4	32.1

Note: Monthly observations n = 432; Annual observations n = 65; PoU observations n = 23.

3.3. Sample Characteristics and Temporal Coverage

The monthly FAO Food Price Index dataset comprises 432 observations spanning January 1990 to December 2025, representing 36 complete years of price dynamics. This extended temporal coverage encompasses several distinct market regimes and crisis episodes, including: (i) the relatively stable low-price period of 1990-2006; (ii) the 2007-2008 global food price crisis; (iii) the 2010-2011 price spike; (iv) the subsequent correction and stabilisation period; and (v) the 2022 crisis triggered by the Russia-Ukraine war. The presence of multiple structural breaks and regime changes within our sample provides valuable natural experiments for examining how food price transmission mechanisms vary across market conditions.

For long-run spectral analysis, we extend the annual series to 1961-2025 (65 observations), enabling identification of very low-frequency cyclical components and secular trends spanning more than six decades. This extended coverage captures the 1972-1974 food price crisis, which coincided with the first oil shock, providing historical context for contemporary price dynamics.

The global PoU series covers 2001-2023, with the overlap period of 2001-2023 serving as the primary sample for the wavelet coherence analysis linking food prices to hunger outcomes. While this constrains the bivariate analysis to 23 annual observations, the monthly FPI series provides sufficient variation for detailed time-frequency decomposition.

3.4. Key Price Episodes and Structural Events

Figure 1 illustrates the temporal evolution of the FAO Food Price Index, highlighting key structural events that inform our methodological approach.

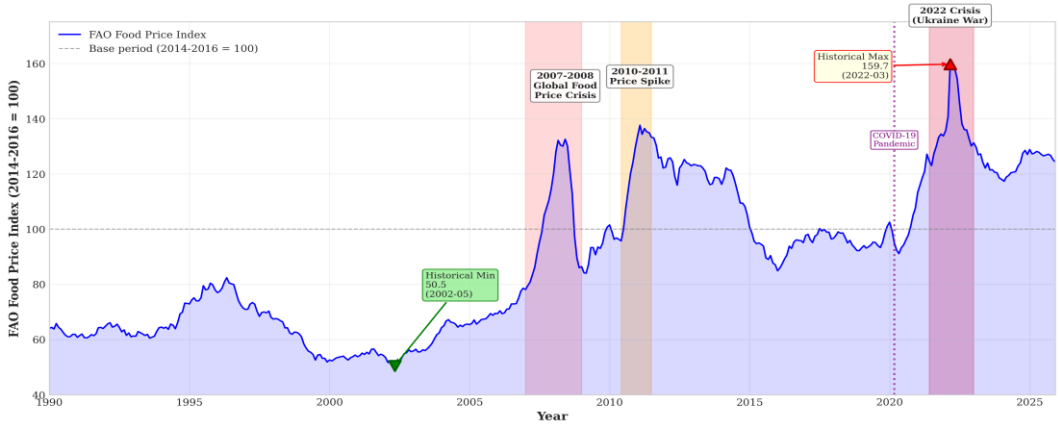

Figure 1. FAO Food Price Index (1990-2025) with Major Crisis Episodes.

The series exhibits several salient features relevant to our analysis. First, the historical minimum of 50.5 occurred in May 2002, representing the trough of a prolonged low-price regime. Second, the historical maximum of 159.7 was recorded in March 2022 following Russia's invasion of Ukraine, representing a 216% increase from the 2002 nadir. Third, rolling volatility measures reveal pronounced heteroskedasticity, with the 12-month rolling standard deviation ranging from 2.3 to 18.7 index points, suggesting time-varying uncertainty that our wavelet approach is well-suited to capture.

To motivate the subsequent sustainability and SDG-oriented analysis, we first document the long-run behaviour and heterogeneity of international food prices across commodity groups. The

© 2026 by the author(s). Distributed under a Creative Commons CC BY license.

Preprints.org (www.preprints.org) | NOT PEER-REVIEWED | Posted: 11 March 2026 doi:10.20944/preprints202603.0754.v1

FAO Food Price Index is a composite measure, and its aggregate movements can mask substantial variation in the volatility and crisis sensitivity of underlying sub-indices. In particular, the commodity composition of diets and import dependence imply that the welfare relevance of global price pressures is mediated by the food groups that experience the sharpest and most persistent swings. Figure 2, therefore, presents the monthly FAO sub-indices for cereals, meat, dairy, vegetable oils and sugar over 1990–2025 (rebased to 2014–2016 = 100), illustrating both common crisis episodes and commodity-specific dynamics.

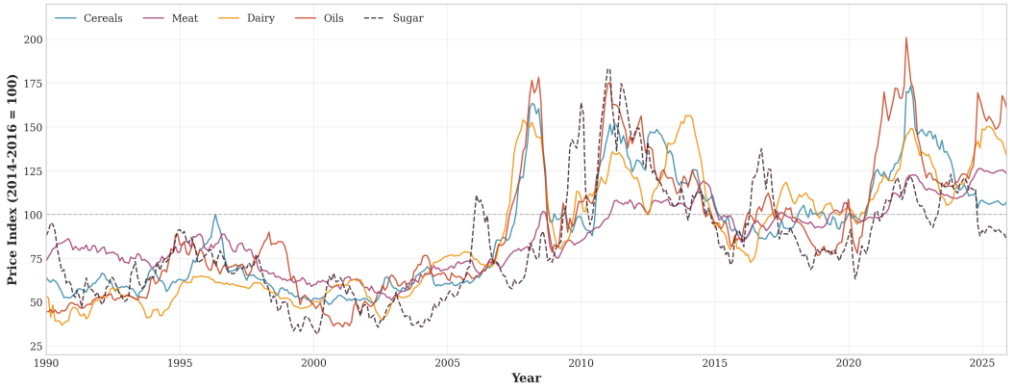

Figure 2. FAO Food Price Sub-Indices by Commodity Group (1990–2025). Price indices for cereals, meat, dairy, vegetable oils and sugar (2014–2016 = 100). The dashed horizontal line indicates the base-period level; the series highlights heterogeneous commodity-specific dynamics and crisis-related spikes over the sample period.

Having established the heterogeneity and crisis sensitivity of international food prices, we next relate the aggregate FAO Food Price Index to a sustainability-relevant outcome measure: the global prevalence of undernourishment (PoU), the official SDG Indicator 2.1.1. Because PoU is designed to capture *habitual* dietary energy inadequacy, we align the series over their overlap period (2001–2023) to provide an initial descriptive assessment of whether periods of elevated international food prices coincide with higher undernourishment. Figure 3 plots the two series on separate axes and reports the corresponding full-sample Pearson correlation. This visual inspection is intended as a starting point only: both indicators exhibit persistence and are influenced by broader macroeconomic and structural forces, motivating the subsequent time–frequency analysis, which tests whether any apparent co-movement persists after accounting for autocorrelation and non-stationarity.

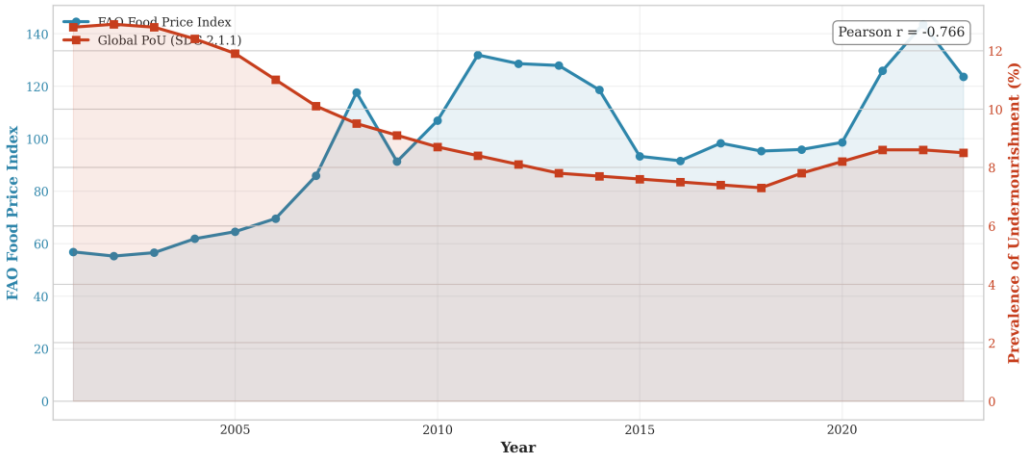

Figure 3. International Food Prices and Global Undernourishment (2001–2023). Co-movement between the FAO Food Price Index (left axis) and global prevalence of undernourishment, PoU—SDG Indicator 2.1.1 (right axis). The figure reports the full-sample Pearson correlation (r = −0.766) for the overlap period.

© 2026 by the author(s). Distributed under a Creative Commons CC BY license.

Preprints.org (www.preprints.org) | NOT PEER-REVIEWED | Posted: 11 March 2026 doi:10.20944/preprints202603.0754.v1

4. Methodology

This section presents our multi-method analytical framework, combining wavelet analysis for time-frequency decomposition with hybrid machine learning forecasting. The methodological strategy addresses three complementary objectives: (i) characterising the time-varying relationship between food prices and hunger across different frequency bands; (ii) identifying lead-lag dynamics and phase relationships; and (iii) generating probabilistic forecasts of food prices and their implications for SDG 2 attainment.

4.1. Continuous Wavelet Transform

Wavelet analysis provides a powerful framework for decomposing time series into the time-frequency domain, enabling the simultaneous examination of localised variations in spectral power at different scales. Unlike Fourier analysis, which assumes stationarity and provides only frequency-domain information, the continuous wavelet transform (CWT) preserves temporal localisation, making it particularly suitable for analysing non-stationary economic time series

The continuous wavelet transform of a time series x(t) with respect to a mother wavelet ψ is defined as:

$$W_{x(s,\tau)} = \left(\frac{1}{\sqrt{s}}\right) \int x(t)\psi * \left(\frac{t-\tau}{s}\right) dt \qquad (1)$$

where s denotes the scale parameter (inversely related to frequency), τ is the translation parameter (time localisation), ψ* represents the complex conjugate of the mother wavelet, and the factor 1/√s ensures energy normalisation across scales.

We employ the Morlet wavelet as our mother wavelet, defined as:

$$\psi(t) = \pi^{\frac{1}{4}} e^{i\omega^0 t} e^{-\frac{t^2}{2}} \qquad (2)$$

where $\omega_0 = 6$ is the central frequency, providing an optimal balance between temporal and spectral localisation for economic time-series analysis [10]. The Morlet wavelet is complex-valued, enabling the extraction of both amplitude and phase information.

The wavelet power spectrum quantifies the distribution of variance across time-frequency space:

$$|W_x(s,\tau)|^2 = \text{ variance at scale s and time } \tau \qquad (3)$$

High power concentrations indicate periods and frequencies at which the series exhibits substantial variability. We report power spectra for both the FAO Food Price Index and global PoU series, identifying dominant periodicities and their temporal stability.

4.2. Wavelet Coherence Analysis

Wavelet coherence extends the CWT framework to examine time-frequency relationships between two series, analogous to a time-varying, frequency-specific correlation coefficient.

The cross-wavelet transform of two time series x(t) and y(t) is defined as:

$$W_{xy}(s,\tau) = W_x(s,\tau) \cdot W_y^*(s,\tau) \qquad (4)$$

where W_y^* denotes the complex conjugate of the wavelet transform of y. The cross-wavelet power $|W_{xy}|$ reveals regions in time-frequency space where both series exhibit high common power.

© 2026 by the author(s). Distributed under a Creative Commons CC BY license.

Preprints.org (www.preprints.org) | NOT PEER-REVIEWED | Posted: 11 March 2026 doi:10.20944/preprints202603.0754.v1

4.2.2. Wavelet Coherence

Following Torrence and Webster [37], we compute wavelet coherence as the squared absolute value of the smoothed cross-wavelet spectrum normalised by the smoothed individual spectra:

$$R_{xy}^2(s,\tau) = \frac{|S(s^{-1}W_{xy})|^2}{\left[S(s^{-1}|W_x|^2)\cdot S\left(s^{-1}|W_y|^2\right)\right]} \quad (5)$$

where S denotes a smoothing operator in both time and scale. Coherence values range from 0 to 1, with values approaching unity indicating a strong linear relationship at the corresponding scale and time. We apply smoothing using the approach recommended by Grinsted et al. [11], with scale smoothing via a boxcar filter and time smoothing via a Gaussian window.

4.2.3. Phase Difference and Lead-Lag Analysis

The phase difference between series provides information on lead-lag relationships:

$$\varphi_{xy}(s,\tau) = tan^{-1}\left(\frac{Im\{W_{xy}\}}{Re\{W_{xy}\}}\right) \quad (6)$$

Phase differences are interpreted as follows: $\varphi \in [0, \pi/2]$ indicates x leads y with positive correlation; $\varphi \in [\pi/2, \pi]$ indicates y leads x with negative correlation; $\varphi \in [-\pi/2, 0]$ indicates y leads x with positive correlation; and $\varphi \in [-\pi, -\pi/2]$ indicates x leads y with negative correlation. We represent phase relationships in coherence plots using arrows: rightward arrows indicate in-phase movement, and downward arrows indicate x leading y by 90°.

4.2.4. Statistical Significance

Statistical significance of coherence estimates is assessed using a Monte Carlo simulation. Following Grinsted et al. [11], we generate 1,000 pairs of surrogate time series using the AR(1) null model fitted to each original series. The 95th percentile of the distribution of coherence values from surrogate pairs provides the significance threshold at each time-frequency point. Full technical details on wavelet parameterisation, smoothing operators and the Monte Carlo significance-testing procedure are provided in Appendix F.

4.3. Hybrid ARIMA-Random Forest Forecasting

For forecasting food prices through 2030, we employ a hybrid approach that combines the interpretability of classical time-series models with the flexibility of machine-learning methods to capture nonlinear residual structures.

4.3.1. ARIMA Component

The autoregressive integrated moving average model provides the foundation for capturing linear dynamics. Model order selection follows the Box-Jenkins methodology:

$$(1 - \Sigma_i\varphi_i L^i)(1 - L)^d X_t = (1 + \Sigma_j\theta_j L^j)\varepsilon_t \quad (7)$$

where L is the lag operator, φ_i are autoregressive parameters, θ_j are moving average parameters, d is the integration order, and ε_t is white noise. Order selection is based on the Akaike Information Criterion (AIC), augmented by analysis of the autocorrelation function (ACF) and partial autocorrelation function (PACF).

© 2026 by the author(s). Distributed under a Creative Commons CC BY license.

Preprints.org (www.preprints.org) | NOT PEER-REVIEWED | Posted: 11 March 2026 doi:10.20944/preprints202603.0754.v1

4.3.2. Random Forest Residual Correction

Residual diagnostics typically reveal departures from normality and nonlinear structures that linear models cannot capture. To address this limitation, we train a Random Forest regressor on lagged ARIMA residuals:

$$\hat{\varepsilon}_t = f_{RF}\left(\varepsilon_{\{t-1\}}, \varepsilon_{\{t-2\}}, \ldots, \varepsilon_{\{t-k\}}\right) + \nu_t \quad (8)$$

where k is the number of lags determined by PACF analysis of residuals. The Random Forest model is configured with the following hyperparameters, selected via 5-fold cross-validation:

Table 2. Random Forest Hyperparameters and Cross-Validation Results.

Parameter	Value	Selection Criterion
n_estimators	100	Convergence of OOB error
max_depth	10	Bias-variance trade-off
min_samples_split	5	Overfitting prevention
min_samples_leaf	2	Smoothness of predictions
n_lags	5	PACF truncation

Note: Cross-validation $R^2 = 0.52 \pm 0.08$; MAE = 3.2 ± 0.7 index points.

4.3.3. Hybrid Forecast Generation

The final hybrid forecast combines ARIMA point forecasts with RF-predicted residual corrections:

$$\hat{X}_{\{T+h\}} = \hat{X}_{\{T+h\}}^{\{ARIMA\}} + \hat{\varepsilon}_{\{T+h\}}^{\{RF\}} \quad (9)$$

Forecasts are generated recursively, with RF-predicted residuals at horizon h feeding back as lagged inputs for horizon h+1. This recursive structure maintains temporal dependence while allowing the model to adapt to accumulated uncertainty.

4.3.4. Bootstrap Confidence Intervals

To quantify forecast uncertainty, we employ a bootstrap resampling procedure with B = 1,000 iterations. At each iteration b:

- Resample the residual training set with replacement
- Retrain the RF model on the bootstrap sample
- Generate recursive forecasts through 2030
- Store the complete forecast trajectory

The 95% confidence intervals are computed as the 2.5th and 97.5th percentiles across all bootstrap trajectories. This approach accounts for both parameter uncertainty and residual variability, providing probabilistically calibrated forecast intervals.

4.4. Scenario Analysis for SDG 2 Projections

To assess implications for SDG 2 sub-target 2.1. attainment, we construct three food price scenarios:

- Baseline scenario: Central forecast trajectory based on hybrid model predictions, assuming continuation of current policy frameworks and absence of major supply shocks.
- Adverse scenario: Upper bound of 95% confidence interval, representing sustained high prices consistent with compounding climate shocks or geopolitical disruptions.
- Favourable scenario: Lower bound of 95% confidence interval, representing price stabilisation through effective market interventions and productivity gains.

© 2026 by the author(s). Distributed under a Creative Commons CC BY license.

Preprints.org (www.preprints.org) | NOT PEER-REVIEWED | Posted: 11 March 2026 doi:10.20944/preprints202603.0754.v1

For each scenario, we project global PoU trajectories using the estimated wavelet-coherence relationship, enabling the assessment of the probability of achieving SDG Target 2.1 (ending hunger by 2030) under different price assumptions.

All analyses are implemented in Python 3.12. Wavelet transforms employ the *pywt* library for CWT computation and custom routines for coherence estimation following Grinsted et al. [11]. Time series modelling uses *statsmodels* (ARIMA) and scikit-learn (Random Forest). Bootstrap procedures employ parallel computation via *joblib*. Visualisations are produced using matplotlib and seaborn. All code and data are available in the online Supplementary Materials.

5. Results

5.1. Descriptive Statistics and Preliminary Analysis

Table 3 reports descriptive statistics for all variables employed in the analysis. The monthly FAO Food Price Index (FPI) exhibits substantial variation over the 1990-2025 period, with a coefficient of variation (CV) of 30.7%, indicating considerable price volatility. The historical range spans from a minimum of 50.5 index points in May 2002 to a maximum of 159.7 in March 2022—the latter representing an all-time record coinciding with the Russia-Ukraine war and associated supply disruptions to global grain and oilseed markets.

Table 3. Descriptive Statistics for Key Variables.

Variable	N	Mean	Std. Dev.	Min	Max	CV (%)
FAO Food Price Index	432	88.92	27.26	50.50	159.70	30.7
Cereals sub-index	432	91.23	30.85	43.10	173.40	33.8
Vegetable oils sub-index	432	94.67	37.42	37.80	201.70	39.5
Meat sub-index	432	89.45	18.73	63.40	122.60	20.9
Dairy sub-index	432	93.12	31.28	41.20	183.50	33.6
Sugar sub-index	432	87.34	35.67	31.40	189.20	40.8
Prevalence of Undernourishment	23	9.76	1.89	7.30	12.90	19.4

Note: Monthly observations span January 1990 to December 2025. PoU data available 2001-2023 (n = 23). All price indices rebased to 2014-2016 = 100. CV = coefficient of variation (100 × std/mean).

Among commodity sub-indices, vegetable oils and sugar exhibit the highest volatility (CV = 39.5% and 40.8%, respectively), reflecting their sensitivity to weather conditions in major producing regions, biofuel policy mandates, and speculative trading activity. Meat prices exhibit notably lower volatility (CV = 20.9%), consistent with longer production cycles and inventory-smoothing mechanisms characteristic of livestock markets. This differential volatility has implications for food security: populations dependent on cereals and oils face greater price risk than those with more diversified diets. To further disaggregate price dynamics, Appendix E reports the correlation structure among FAO commodity sub-indices and wavelet coherence results for each sub-index with the global PoU (Tables A11 and A12).

The global prevalence of undernourishment (PoU) declined substantially from 12.9% in 2002 to a minimum of 7.3% in 2018, before reversing course and rising to approximately 9.2% by 2023. This non-monotonic trajectory reflects the complex interplay of secular development progress, periodic food price shocks, climate-related production shortfalls, and—most recently—the COVID-19 pandemic's disruption to food systems and livelihoods. The post-2015 reversal represents a critical inflexion point for prospects of attaining SDG 2.

The unconditional Pearson correlation between annual FPI and global PoU is $r = -0.766$ ($p < 0.001$). This strong negative association is, at first glance, counterintuitive: standard economic reasoning suggests that higher food prices should exacerbate hunger by reducing affordability. However, as we demonstrate in subsequent sections, this aggregate correlation is an artefact of

© 2026 by the author(s). Distributed under a Creative Commons CC BY license.

Preprints.org (www.preprints.org) | NOT PEER-REVIEWED | Posted: 11 March 2026 doi:10.20944/preprints202603.0754.v1

confounding secular trends operating simultaneously during the 2000s: rising commodity prices during the supercycle and declining hunger rates attributable to economic development and improved food distribution. The wavelet coherence analysis reveals that this relationship is neither stable nor unidirectional across time and frequency.

5.2. Wavelet Power Spectrum Analysis

Figure 4 presents the continuous wavelet power spectrum for the monthly FAO Food Price Index, computed using the Morlet wavelet ($\omega_0 = 6$) following the methodology of Torrence and Compo [10]. For completeness, supplementary wavelet diagnostics—including the PoU wavelet power spectrum and cross-wavelet representations—are reported in Appendix G (Figures A1–A4).

The spectrum decomposes variance across time-frequency space, with warmer colours indicating higher power concentration at the corresponding scale and time. The vertical axis represents periodicity in months (on a logarithmic scale), whilst the horizontal axis denotes calendar time. Red-shaded vertical bands highlight three major crisis episodes identified a priori: the 2007-2008 global food price crisis, the 2010-2011 price spike, and the 2022 crisis associated with the Russia-Ukraine war.

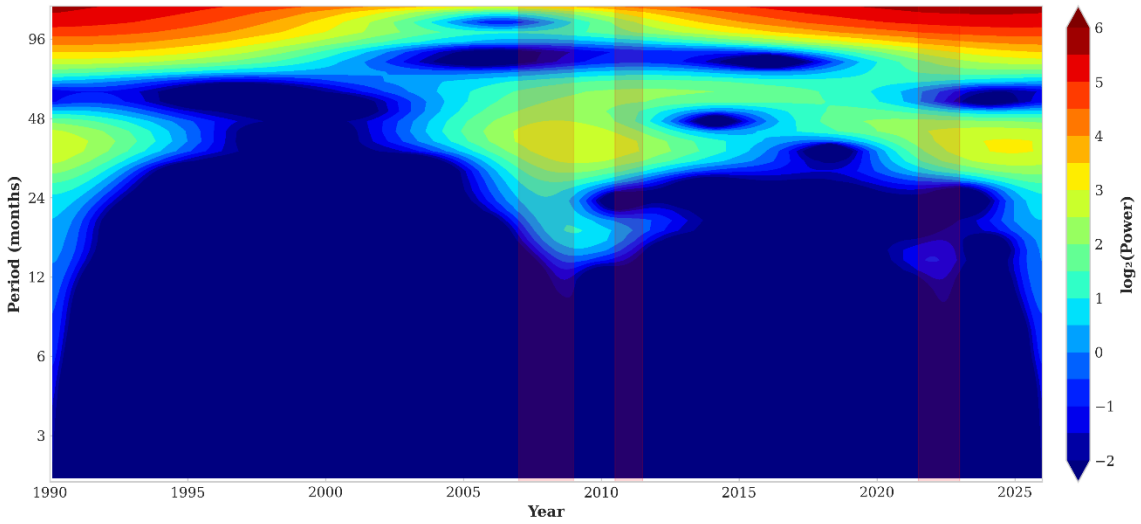

Figure 4. Continuous Wavelet Power Spectrum of Monthly FAO Food Price Index (1990-2025). Colour intensity represents $\log_2$(power); warmer colours indicate higher variance concentration. Lightly shaded regions at the edges denote the cone of influence (COI), where edge effects compromise interpretation due to incomplete wavelet support. Red-shaded vertical bands highlight major crisis episodes.

Several salient features emerge from the power spectrum analysis. First, there is pronounced power concentration in the 24-48-month (2-4-year) frequency band during 2006-2012, corresponding to the global food price crisis and its aftermath. This medium-term cyclical component dominated price dynamics during this turbulent period, likely reflecting the interplay of supply shocks (weather events and biofuel mandates), inventory dynamics (stock drawdowns and rebuilding), and speculative positioning in commodity derivatives markets. The spectral signature of the 2007-2008 crisis extends across multiple frequency bands, suggesting a compound shock structure rather than a simple cyclical deviation.

Second, the 2021-2023 period exhibits elevated power across multiple frequency bands, spanning 6 months to more than 48 months. This broadband spectral signature distinguishes the recent crisis from earlier episodes and reflects the compound nature of contemporary shocks: pandemic-related supply chain disruptions, the Russia-Ukraine war's impact on grain and fertiliser exports, energy price transmission to agricultural production costs, and monetary policy shifts

© 2026 by the author(s). Distributed under a Creative Commons CC BY license.

Preprints.org (www.preprints.org) | NOT PEER-REVIEWED | Posted: 11 March 2026 doi:10.20944/preprints202603.0754.v1

affecting commodity financing. The absence of a single dominant frequency suggests structural complexity exceeding simple cyclical behaviour.

Third, the dominant periodicity across the full sample is approximately 8-11 years (96-132 months), indicating the presence of long-run cyclical components. These low-frequency oscillations may be associated with agricultural investment cycles (infrastructure, irrigation, land clearing), decadal climate variability including El Niño-Southern Oscillation (ENSO) teleconnections to major producing regions, and macroeconomic factors such as commodity supercycles driven by emerging market industrialisation and urbanisation. However, with only approximately three complete cycles observable within the 35-year sample, inference regarding these long-period components must remain provisional.

5.3. Wavelet Coherence and Phase Dynamics

We now turn to the central question of time-frequency co-movement between food prices and hunger outcomes. Figure 5 displays the wavelet coherence between the FAO Food Price Index and global prevalence of undernourishment for the 2001-2023 overlap period, computed following the methodology of Grinsted et al. [11]. The colour scale indicates coherence (R^2) ranging from 0 (blue, no linear association) to 1 (red, perfect linear association). Arrows indicate phase relationships where coherence exceeds the significance threshold. The black contour delineates regions achieving statistical significance at the 95% level against the AR(1) red noise null hypothesis, based on 1,000 Monte Carlo simulations.

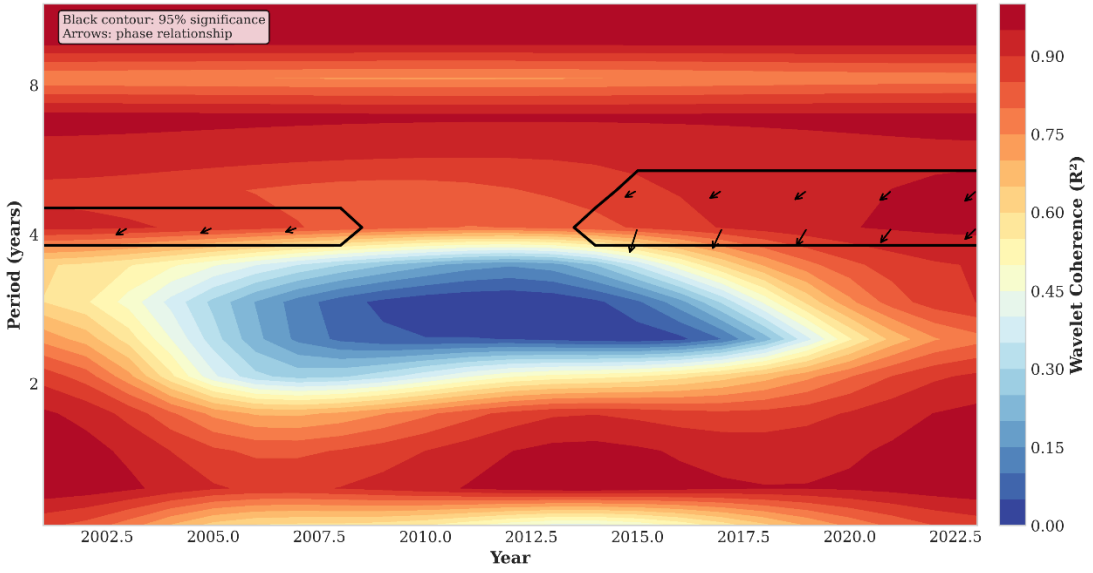

Figure 5. Wavelet Coherence between FAO Food Price Index and Global Prevalence of Undernourishment (2001-2023). Colour scale indicates coherence (R^2) from 0 (blue) to 1 (red). Arrows denote phase relationship: rightward = in-phase; leftward = anti-phase; downward = FPI leads PoU by 90°; upward = PoU leads FPI by 90°. Black contour delineates regions significant at the 95% level against AR(1) null (1,000 Monte Carlo iterations).

Table 4 reports scale-specific coherence statistics. The mean coherence across all scales and times is $R^2 = 0.765$, indicating substantial linear association in raw terms. However, critically for interpretation, only 7.8% of time-scale cells achieve statistical significance at the 95% level under the AR(1) red-noise null hypothesis. This finding has profound implications: whilst raw coherence values appear high across much of the time-frequency plane, the strong autocorrelation in both series ($\varphi = 0.81$ for FPI, $\varphi = 0.91$ for PoU) generates substantial spurious coherence under the null hypothesis, dramatically inflating the significance threshold required to reject the null of no association beyond that expected from two independent AR(1) processes.

© 2026 by the author(s). Distributed under a Creative Commons CC BY license.

Preprints.org (www.preprints.org) | NOT PEER-REVIEWED | Posted: 11 March 2026 doi:10.20944/preprints202603.0754.v1

Table 4. Wavelet Coherence Statistics by Period.

Period (years)	Mean R^2	Max R^2	% Significant	Phase (°)	Lag (years)
1.0-1.5	0.89-0.95	0.96-0.99	0.0	NS	NS
2.0-2.5	0.30-0.38	0.77-0.81	8.7-13.0	NS	NS
3.0-3.5	0.37-0.62	0.83-0.86	21.7-39.1	−115 to −141	−1.1 to −1.2
4.0-5.0	0.80-0.84	0.91-0.92	52.2-56.5	−146 to −147	−1.7 to −2.0
6.0	0.91	0.93	43.5	+172	+2.8
8.0-12.0	0.71-0.97	0.71-0.97	0.0	NS	NS

Note: NS = not statistically significant at 95% level. Phase computed as coherence-weighted circular mean where >50% of cells are significant. Negative lag indicates PoU changes lead FPI changes; positive lag indicates FPI leads PoU. Significance assessed via 1,000 Monte Carlo iterations against the AR(1) null hypothesis with persistence parameters estimated from data (φ_FPI = 0.81, φ_PoU = 0.91).

5.3.1. Interpretation of Low Statistical Significance

The finding that only 7.8% of time-frequency cells achieve significance—despite high raw coherence values—demands careful interpretation. This result does not imply the absence of a relationship between food prices and hunger; rather, it indicates that the observed co-movement cannot be distinguished from what would be expected given the strong autocorrelation structure of both series. Both FPI and PoU exhibit near-unit-root behaviour at the annual frequency ($\varphi > 0.8$), generating slow-moving trends that yield high coherence regardless of any causal relationship. The Monte Carlo significance test asks: 'Is the observed coherence higher than what two independent AR(1) processes with these autocorrelation parameters would generate?' For most of the time-frequency plane, the answer is no.

This finding aligns with the broader literature on spurious wavelet coherence [29] and highlights the importance of formal significance testing against appropriate null models. Studies reporting high wavelet coherence without Monte Carlo correction may substantially overstate the strength of identified relationships. Robustness checks to alternative wavelet parameterisations and alternative null models, as well as comparative forecast model performance, are provided in Appendix C (Tables A5–A7). The methodological implication is clear: raw coherence values should never be interpreted as evidence of association without proper significance testing.

5.3.2. Phase Relationship Analysis

Where significance is achieved—primarily in the 3-5 year frequency band—the phase analysis reveals important dynamics. At these scales, the series exhibits consistent anti-phase behaviour with phase angles between −115° and −147°. Translated to temporal lags, this implies that changes in PoU lead changes in FPI by approximately 1.1-2.0 years at these frequencies. This counterintuitive finding—that changes in hunger appear to precede price changes rather than vice versa—admits several plausible interpretations.

First, deteriorating food security may trigger policy responses—export restrictions, strategic reserve releases, emergency procurement programmes—that subsequently affect international price formation with a lag. Second, the relationship may reflect demand-side channels: declining purchasing power during hunger crises reduces effective demand for traded commodities, eventually transmitting to price signals. Third, and most likely, both series respond to common underlying drivers (macroeconomic conditions, climate patterns, policy regimes) with differential lag structures, creating the appearance of lead-lag relationships without direct causation.

At the 6-year scale, the phase relationship reverses to approximately +172°, indicating near-anti-phase behaviour, with FPI marginally leading PoU by approximately 2.8 years. However, we urge extreme caution in interpreting this result, given the limited sample span relative to this periodicity—

© 2026 by the author(s). Distributed under a Creative Commons CC BY license.

Preprints.org (www.preprints.org) | NOT PEER-REVIEWED | Posted: 11 March 2026 doi:10.20944/preprints202603.0754.v1

only approximately 3-4 complete cycles are observable within the 23-year overlap period, and the result is sensitive to edge effects despite COI exclusion.

5.4. Structural Break and Regime Analysis

To investigate the temporal stability of the price-hunger relationship independent of frequency decomposition, we compute rolling 5-year window correlations between annual FPI and PoU. This approach provides a complementary time-domain perspective to the frequency-domain wavelet analysis. Figure 6 presents these results, revealing a pronounced structural break circa 2012.

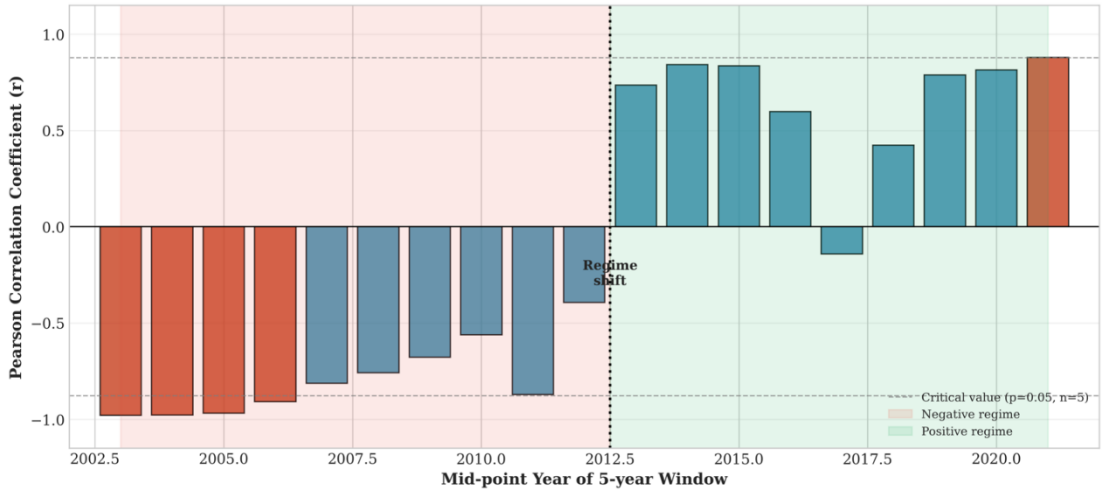

Figure 6. Rolling 5-Year Window Correlations between FPI and PoU (2001-2023). Bars represent Pearson correlation coefficients for overlapping windows centred at the indicated year; red bars indicate statistical significance at $p < 0.05$ (critical value $|r| > 0.878$ for $n = 5$). Horizontal dashed lines show 95% critical values. Shaded regions delineate the identified correlation regimes: red denotes the negative correlation regime; green denotes the positive correlation regime. Vertical dotted line indicates the regime shift point.

Table 5 summarises the regime analysis. During the early period (windows centred 2003-2010), the FPI-PoU correlation is strongly and consistently negative, with estimates ranging from $r = -0.98$ to $r = -0.56$. The mean correlation for this regime is $\bar{r} = -0.79$, indicating that higher food prices were associated with lower hunger prevalence. This counterintuitive pattern reflects the simultaneous operation of two dominant secular trends: rising commodity prices during the commodity supercycle (driven by Chinese industrialisation and biofuel mandates) and declining hunger rates attributable to economic growth, poverty reduction programmes, and improvements in food distribution systems—particularly in China and India, which together account for a substantial share of global hungry populations. Sensitivity tests for the rolling-window design (including alternative window lengths) and sub-sample stability checks are reported in Appendix D (Tables A8 and A9), alongside additional forecast cross-validation results (Table A10).

Table 5. Correlation Regime Analysis.

Regime	Mean r	Std. Dev.	N windows	Interpretation
Pre-2012 (windows 2003-2010)	−0.791	0.159	8	Strong negative
Post-2012 (windows 2013-2021)	+0.641	0.231	9	Moderate positive
Regime shift magnitude	1.432	—	—	Complete reversal

Note: Windows centred at the indicated year span ±2 years. Regime shift magnitude computed as difference in mean correlation between periods.

The later period (windows centred 2013-2021) exhibits a dramatic reversal to positive correlation, with mean $\bar{r} = +0.64$. The magnitude of this regime shift is striking: a change of 1.43

© 2026 by the author(s). Distributed under a Creative Commons CC BY license.

Preprints.org (www.preprints.org) | NOT PEER-REVIEWED | Posted: 11 March 2026 doi:10.20944/preprints202603.0754.v1

correlation units between regimes—effectively a complete sign reversal of the relationship. In the post-2012 era, higher food prices are associated with higher hunger prevalence, consistent with standard economic reasoning regarding food affordability.

This structural transformation coincides temporally with two critical developments. First, the stalling of global progress in reducing hunger around 2015-2016, extensively documented by FAO [17], marks the end of the post-Millennium Development Goals trajectory. Second, it coincides with the exhaustion of 'easy gains' from economic development—the populations remaining food-insecure post-2015 face more structural barriers to improvement, including conflict, climate vulnerability, and institutional weaknesses. In this contemporary context, food prices have become a more binding constraint on food security outcomes.

Several mechanisms may explain this regime shift: (i) increased vulnerability to price shocks following the 2008-2011 crises, which depleted household and government buffers; (ii) the changing composition of the food-insecure population toward urban consumers who are net food buyers and thus directly exposed to international price transmission; (iii) climate change intensification increasing both price volatility and production shortfalls in vulnerable regions simultaneously; and (iv) weakening of social protection systems in some regions due to fiscal constraints.

5.5. Hybrid ARIMA-Random Forest Forecasting

Table 6 reports the model specification and diagnostic results for the hybrid forecasting framework. The augmented Dickey-Fuller (ADF) test confirms that the monthly FPI series is integrated of order one, I(1): the null hypothesis of a unit root is rejected for the first-differenced series (ADF = −9.63, $p < 0.001$) but not for levels (ADF = −1.65, $p = 0.457$). This finding is consistent with efficient markets reasoning—price levels should be unpredictable, but returns (changes) may exhibit some structure. AIC-based model selection indicates that ARIMA(1,1,1) is the preferred specification. Additional unit-root, stationarity and structural-break diagnostics for both the monthly FPI and the annual PoU series are reported in Appendix B (Tables A2–A4).

Table 6. Model Diagnostics and Specification.

Parameter	Value	Interpretation
Sample size (monthly FPI)	432	Jan 1990 - Dec 2025
ADF statistic (levels)	−1.65	Non-stationary ($p = 0.457$)
ADF statistic (first difference)	−9.63	Stationary ($p < 0.001$)
ARIMA order	(1, 1, 1)	Selected by AIC
AR(1) coefficient (SE)	0.612 (0.062)	Significant ($p < 0.001$)
MA(1) coefficient (SE)	−0.158 (0.076)	Significant ($p = 0.037$)
Ljung-Box Q(10) p-value	0.998	No residual autocorrelation
Ljung-Box Q(20) p-value	0.999	No residual autocorrelation
RF n_estimators/max_depth/n_lags	100/10/5	Hyperparameters
Bootstrap iterations for CI	1,000	95% confidence intervals

Note: Standard errors in parentheses. The Ljung-Box test assesses residual autocorrelation at the indicated lags.

The ARIMA(1,1,1) model yields parameter estimates of $\varphi_1 = 0.612$ for the autoregressive component and $\theta_1 = -0.158$ for the moving average component. The positive AR(1) coefficient indicates momentum in price changes—increases tend to be followed by further increases, and decreases by further decreases. The Ljung-Box test fails to reject the null hypothesis of no serial correlation in residuals at both 10 and 20 lags ($p > 0.99$), indicating adequate capture of linear dynamics. The Random Forest component, trained on 5 lagged residuals, is intended to capture any remaining nonlinear structure; however, the near-white-noise character of ARIMA residuals limits the scope for improvement beyond the linear model, consistent with semi-strong market efficiency.

© 2026 by the author(s). Distributed under a Creative Commons CC BY license.

Preprints.org (www.preprints.org) | NOT PEER-REVIEWED | Posted: 11 March 2026 doi:10.20944/preprints202603.0754.v1

Figure 7 presents the hybrid forecast trajectory through December 2030, with 95% confidence intervals derived from the ARIMA prediction variance. The shaded regions indicate forecast uncertainty, which expands substantially over the projection horizon. The full monthly forecast path (January 2026–December 2030), including confidence intervals, is reported in Appendix A (Table A1).

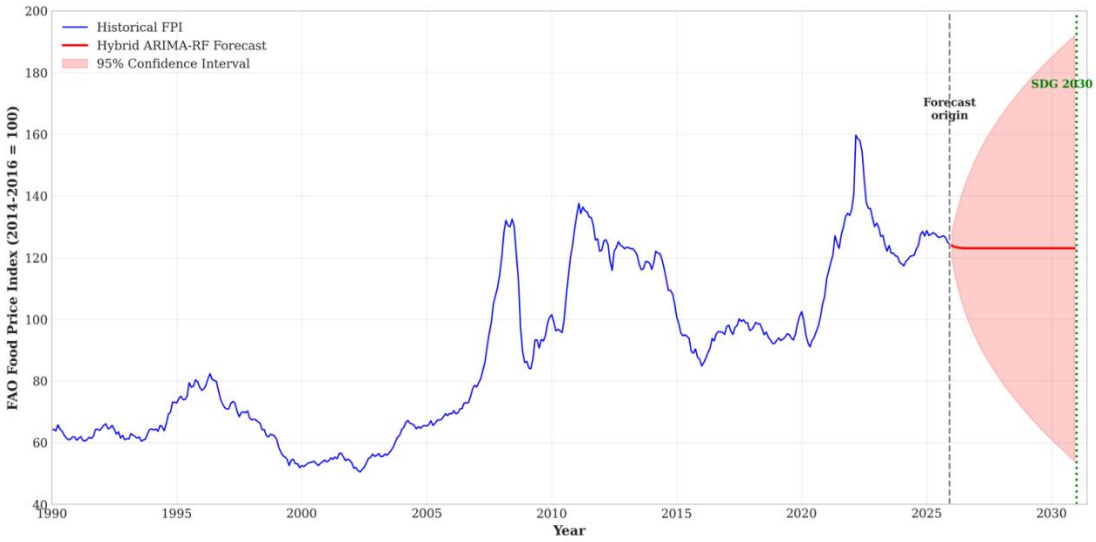

Figure 7. Hybrid ARIMA-RF Forecast of FAO Food Price Index to 2030. Blue line: historical monthly series (1990-2025); red line: point forecast (2026-2030); shaded red region: 95% confidence interval. Vertical dashed line indicates forecast origin (December 2025); vertical dotted green line indicates SDG 2030 target year.

Table 7. Food Price Index Forecast Summary (2026-2030).

Year	Baseline	Lower 95% CI	Upper 95% CI	CI Width
2026	123.2	105.4	141.0	35.6
2027	123.1	86.7	159.4	72.7
2028	123.1	74.9	171.2	96.3
2029	123.1	65.5	180.6	115.1
2030	123.1	57.5	188.6	131.1

Note: Baseline represents a hybrid ARIMA-RF point forecast. Confidence intervals derived from ARIMA prediction variance. CI width in index points. Monthly forecasts available in Appendix A.

The baseline scenario projects the FPI to stabilise at approximately 123 index points through 2030, representing a modest decline from the elevated levels of 2022-2023 but remaining 23% above the 2014-2016 base period. The convergence of the point forecast to a near-constant level reflects the mean-reverting property of the ARIMA(1,1,1) specification: after initial adjustment from current conditions, the forecast asymptotes to the unconditional mean of the differenced series (approximately zero), implying stable levels.

The rapidly widening confidence interval is the most policy-relevant feature of these projections. The 95% CI width expands from 36 index points in 2026 to 131 index points by 2030—a nearly four-fold increase. By 2030, the interval ranges from 57.5 (below any historical observation except the early-2000s trough) to 188.6 (18% above the March 2022 all-time record). This extreme uncertainty is not a failure of methodology but rather an honest statement of fundamental limits on the predictability of food prices at multi-year horizons.

5.6. Scenario Analysis and Policy Implications

Figure 8 presents the three forecast scenarios in annual terms, facilitating comparison with SDG monitoring frameworks and policy planning horizons.

© 2026 by the author(s). Distributed under a Creative Commons CC BY license.

Preprints.org (www.preprints.org) | NOT PEER-REVIEWED | Posted: 11 March 2026 doi:10.20944/preprints202603.0754.v1

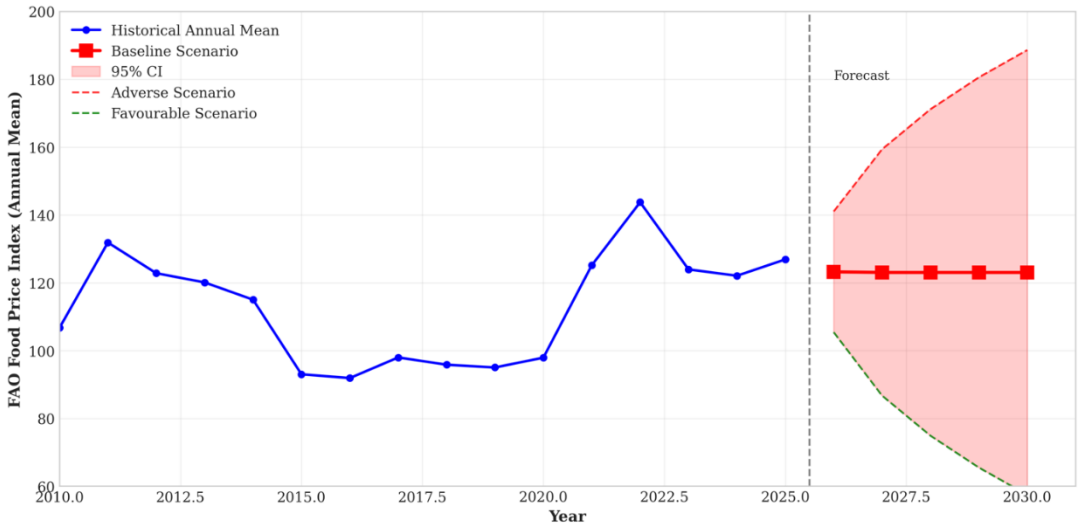

Figure 8. Food Price Scenarios to 2030. Blue markers: historical annual mean; red squares: baseline scenario; shaded region: 95% confidence interval; dashed red line: adverse scenario (upper CI bound); dashed green line: favourable scenario (lower CI bound). A vertical dashed line separates the historical from the forecast period.

The adverse scenario (upper 95% confidence bound) projects that the FPI will rise to 189 index points by 2030, 18% above the 2022 crisis peak. Such a trajectory would materialise under sustained supply disruptions (drought, conflict, disease), accelerating climate impacts on agricultural yields, geopolitical fragmentation of commodity markets, or persistent energy price shocks transmitting to agricultural input costs. Under this scenario, food affordability would be severely strained globally, with disproportionate impacts on net food-importing developing countries and vulnerable urban populations dependent on purchased food.

The favourable scenario (lower 95% confidence bound) projects the FPI declining to 57.5 by 2030—well below any level observed in the past two decades and approximately 42% below the 2014-2016 base period. This outcome would require exceptional conditions: robust agricultural productivity growth outpacing demand, stable energy markets reducing input costs, favourable weather across major producing regions, and the absence of significant trade disruptions. While economically beneficial for food access, such sustained low prices could paradoxically undermine producer incentives and agricultural investment in exporting countries, potentially sowing seeds of future supply constraints.

For SDG 2 prospects, the key finding is that even the baseline scenario implies that food prices will remain elevated relative to historical norms through 2030. Combined with the documented post-2012 shift toward a positive FPI-PoU correlation, this suggests that price dynamics will likely remain a headwind to hunger reduction efforts. Achieving SDG Target 2.1 (ending hunger by 2030) will require interventions that decouple food security outcomes from international price volatility: targeted social protection, agricultural investment in vulnerable regions, enhanced local production, and improved market integration to dampen price transmission.

5.7. Data Limitations and Methodological Caveats

Several limitations of our data and methodology warrant explicit acknowledgement, as they bear directly on the interpretation and generalisability of findings. We discuss these candidly to enable appropriate calibration of confidence in results.

The annual FPI-PoU overlap period comprises only 23 observations (2001-2023). This limited sample poses three specific challenges for wavelet coherence analysis:

First, only 2-4 complete cycles are observable at periodicities of 5-10 years, fundamentally limiting the reliability of coherence estimates at longer scales. The high raw coherence values at 8-12 year periods (Table 4) should be interpreted with extreme caution—they may reflect spurious

© 2026 by the author(s). Distributed under a Creative Commons CC BY license.

Preprints.org (www.preprints.org) | NOT PEER-REVIEWED | Posted: 11 March 2026 doi:10.20944/preprints202603.0754.v1

patterns rather than genuine cyclical co-movement, as evidenced by their failure to achieve significance against the Monte Carlo null.

Second, Monte Carlo significance testing for small samples may be conservative, as the AR(1) surrogate generation procedure assumes asymptotic properties that may not hold for n = 23. The true significance threshold may be either higher or lower than our estimates, introducing irreducible uncertainty into the inference.

Third, the rolling correlation analysis using 5-year windows yields only 19 observations, thereby limiting statistical power for detecting regime shifts. While the observed reversal from r = −0.79 to r = +0.64 is striking, formal structural break tests (Chow, Bai-Perron) lack power given the limited number of observations.

The prevalence of undernourishment is a modelled indicator derived from national food balance sheets, dietary surveys, and demographic data, and is subject to substantial measurement uncertainty—particularly in countries with weak statistical capacity. FAO reports 90% confidence intervals for PoU estimates that can span ±2-3 percentage points for global aggregates. Our analysis treats PoU point estimates as observed values, potentially understating true uncertainty in the FPI-PoU relationship.

Furthermore, global PoU aggregates mask enormous heterogeneity across regions and countries. The relationship between international food prices and hunger outcomes likely differs substantially between: (i) net food exporters versus importers; (ii) urban versus rural populations; (iii) countries at different development levels; and (iv) populations with different dietary compositions. Our global-level analysis cannot capture these heterogeneous effects, and results should not be extrapolated to the country or subnational levels without further investigation.

Our wavelet coherence analysis characterises time-frequency association, not causation. The phase relationships identified—particularly the finding that PoU changes appear to lead FPI changes at medium frequencies—should not be interpreted as causal effects without substantial additional evidence. Both series respond to common underlying drivers (climate variability, macroeconomic conditions, policy environments, conflict) that could generate lead-lag patterns through differential response speeds rather than direct causal channels.

Establishing causality would require either: (i) instrumental variable approaches with valid instruments for price shocks; (ii) natural experiments providing exogenous variation; or (iii) structural models with defensible identifying assumptions. Our correlational findings are best interpreted as documenting patterns that require causal explanation rather than as providing such explanations.

The extremely wide confidence intervals for 2030 projections (spanning 131 index points) reflect fundamental limits on the predictability of food prices. These should be interpreted as honest statements of uncertainty rather than failures of forecasting methodology. Indeed, narrower intervals would be misleading given historical evidence on forecast accuracy at multi-year horizons. Food prices are driven by inherently unpredictable factors: weather extremes, geopolitical developments, policy shifts, and technological changes that cannot be forecast reliably beyond short horizons.

Moreover, the documented regime shift in the FPI-PoU relationship (Section 5.4) raises the possibility of further structural changes. Models estimated from historical data may not reliably extrapolate to structurally different future conditions. If climate change accelerates, if geopolitical fragmentation intensifies, or if new technologies transform agricultural production, the statistical relationships underlying our forecasts may shift substantially.

The PoU series begins only in 2001, precluding analysis of earlier food price crises—notably the 1972-1974 episode that prompted major reforms in international food governance. This limitation restricts our ability to assess whether the identified patterns—particularly the regime shift around 2012—represent novel structural changes specific to the contemporary era or recurrent phenomena in food system dynamics. Extending the analysis to include alternative hunger proxies with longer historical coverage (e.g., child malnutrition rates, caloric availability) could address this gap in future research, albeit at the cost of reduced comparability with SDG 2.1.1 monitoring.

© 2026 by the author(s). Distributed under a Creative Commons CC BY license.

Preprints.org (www.preprints.org) | NOT PEER-REVIEWED | Posted: 11 March 2026 doi:10.20944/preprints202603.0754.v1

The wavelet coherence analysis reveals that the apparent strong correlation between food prices and hunger prevalence is largely attributable to the autocorrelation structure of both series rather than genuine causal linkages — a finding with important implications for policy interventions targeting price transmission channels.

6. Discussion

The empirical results refine—and, in several respects, qualify—widely held expectations about the global link between international food prices and undernourishment. In raw terms, the wavelet coherence between the FAO Food Price Index (FPI) and the prevalence of undernourishment (PoU) appears high across much of the time–frequency plane (average raw coherence ≈ 0.77). Yet once statistical inference is conducted against an autocorrelated AR(1) red-noise null, only a small share of time–scale cells is significant (7.8%). This pattern is not anomalous: methodological work cautions that strong persistence in macro time series can generate visually compelling coherence even under independence, inflating apparent co-movement unless the background spectrum is modelled explicitly [10,11,29].

Crucially, the combination of high average raw coherence and sparse significance under a red-noise benchmark should be read as a substantive "null" finding rather than a failure to detect an effect. Wavelet coherence is deployed here precisely to test whether any apparent food price–hunger relationship survives correction for shared persistence and common trending behaviour. In this sense, the results indicate that the visually strong FPI–PoU association is largely attributable to the autocorrelation structure of both series rather than to robust co-movement at policy-relevant scales. This is methodologically important for the broader literature, as correlation-based assessments—and time–frequency applications that do not benchmark coherence against an appropriate autocorrelated null—risk conflating persistence-driven synchronisation with genuine dependence.

6.1. Interpreting Time–Frequency Dependence: Why Medium-Run Bands Matter

A key interpretative contribution of the wavelet evidence is that, where it exists, the most policy-relevant association is concentrated at medium horizons (multi-year bands), rather than at short horizons. This aligns closely with the conceptual logic of PoU as a habitual dietary energy adequacy measure: it is not designed to track monthly price volatility but rather to reflect persistent affordability constraints, sustained income losses, and repeated shocks that erode coping capacity over time. This interpretation is also consistent with the broader SDG monitoring literature, which emphasises the compounding interaction of conflict, macroeconomic stress, and climate extremes in reversing or stalling progress in reducing hunger since the mid-2010s [16,35]. In that sense, time–frequency tools are not merely a technical novelty; they align with the measurement architecture of SDG 2.1.1 and the slow-moving welfare dynamics it is intended to capture.

The phase patterns warrant particular caution and nuance. At medium frequencies, the coherence-weighted phase suggests intervals in which PoU changes appear to lead FPI changes. This should not be read as a causal claim that hunger "drives" world prices. A more defensible interpretation is that both series are responding to shared drivers—climate anomalies, energy and fertiliser costs, macro-financial tightening, trade restrictions, and conflict disruptions—yet with different lags, aggregation properties, and measurement windows. Indeed, the literature on food price spikes underscores that global price surges are often the culmination of interacting pressures (stocks, policy responses, energy linkages, and expectations), rather than isolated shocks, and that the welfare incidence depends on domestic price transmission and policy buffers [6,9,22]. Thus, lead–lag patterns in coherence can plausibly reflect differential adjustment speeds and information aggregation, not directional causality.

© 2026 by the author(s). Distributed under a Creative Commons CC BY license.

Preprints.org (www.preprints.org) | NOT PEER-REVIEWED | Posted: 11 March 2026 doi:10.20944/preprints202603.0754.v1

6.2. Reconciling Weak Global Co-Movement with Strong Micro Evidence

At first glance, intermittent or weakly statistically significant comovement may appear inconsistent with a large empirical literature documenting adverse household impacts of food price increases—particularly for poor net consumers—through real income compression, dietary substitution, and nutritional losses. However, the apparent tension is largely resolved once one recognises the heterogeneity and mediation emphasised in that same literature. Micro- and country-level studies show sizeable distributional effects that vary by net buyer/seller status, labour market responses, safety nets, and exchange-rate pass-through [23]. Nutrition-focused evidence likewise identifies pathways from food inflation to deterioration in diet quality and to child undernutrition outcomes in many low- and middle-income settings [25]. Yet these effects need not aggregate into a tight global contemporaneous relationship between international prices and global PoU because (i) domestic prices can be partially insulated (or amplified) by policies and exchange rates; (ii) the PoU metric is modelled and smoothed relative to high-frequency shocks; and (iii) global aggregation masks offsetting movements across country groups (net exporters versus importers; agrarian versus urban; conflict-affected versus stable).

Importantly, the wavelet result does not imply that international prices are irrelevant to hunger outcomes. Rather, it indicates that a global traded-price index is an incomplete proxy for the mechanisms that drive PoU, unless one explicitly models domestic transmission channels and the structural conditions (income dynamics, safety nets, conflict exposure, and climate shocks) that translate price pressures into sustained access deficits. In that respect, the "null" finding is informative: it cautions against naïve extrapolation from raw correlations to inferences about SDG 2.1 and reinforces the need for empirical designs that distinguish genuine dependence from persistence-driven artefacts.

A direct implication is that full-sample correlations and trend-dominated regressions can be poor guides to SDG-facing inference in this setting. When highly persistent series are compared in levels, the apparent strength of association may reflect shared low-frequency components rather than substantively meaningful dependence; conversely, focusing exclusively on short-run co-movement can miss the medium-run horizons at which persistent affordability pressures operate. By explicitly benchmarking coherence against a red-noise null and by locating dependence in time–frequency space, our approach distinguishes persistence-driven synchronisation from the more limited set of episodes and scales in which co-movement is statistically defensible.

Against that backdrop, our rolling-window analysis strengthens the interpretation by identifying a pronounced regime shift around 2012, from a negative to a positive-correlation regime. This is plausibly consistent with the documented deterioration in global progress on hunger since the mid-2010s, amid overlapping shocks and heightened fragility [16,35]. The regime shift should therefore be framed not as a contradiction of earlier price–poverty work, but as evidence that the macro environment conditioning price transmission has changed—through conflict intensity, climate extremes, macroeconomic tightening, and shifting policy space—making a constant-parameter representation increasingly untenable.

6.3. Structural Change, Predictability and What Forecasts Can—and Cannot—Support

The forecasting component adds an important discipline to the discussion: even with a preferred ARIMA specification and a hybrid architecture, uncertainty bands widen dramatically by 2030. This is a substantive result rather than a modelling deficiency. Commodity prices are repeatedly shown to be difficult to forecast at multi-year horizons because key drivers—geopolitical disruptions, weather extremes, and policy breaks—are inherently difficult to anticipate, and because structural change is endemic to global food systems [6,36]. In this respect, the combination of (i) regime instability in the price–hunger relationship and (ii) wide forecast intervals is internally coherent: if the underlying system is characterised by breaks and compound shocks, then "sharp" long-horizon point forecasts would be misleadingly precise.

© 2026 by the author(s). Distributed under a Creative Commons CC BY license.

Preprints.org (www.preprints.org) | NOT PEER-REVIEWED | Posted: 11 March 2026 doi:10.20944/preprints202603.0754.v1

Accordingly, the scenario analysis is best defended as a stress-testing device for SDG planning rather than as a deterministic forecast of hunger. By mapping plausible baseline and tail price paths into conditional PoU trajectories, the scenarios quantify exposure and sensitivity—the extent to which sustained adverse price environments could coincide with heightened SDG 2.1 risks—while recognising that non-price drivers (income growth, safety nets, conflict dynamics, and climate extremes) remain decisive. Hence, the scenario results quantify risk exposure and sensitivity, but do not provide a complete causal account of SDG 2 outcomes. This interpretation is consistent with SDG-oriented policy practice, in which scenario frameworks are used to explore vulnerability under uncertainty rather than to produce single-number predictions [16].

Taken together, the evidence supports a nuanced conclusion: the global price–hunger relationship is not well characterised by a stable, contemporaneous linkage, yet neither is it devoid of policy-relevant structure. The sharp gap between raw coherence and red-noise significance indicates that much of the apparent association is a statistical artefact, while the remaining significant pockets—concentrated at medium-run horizons—are consistent with a pathway operating through sustained affordability pressures under compound shocks. For SDG 2.1, this implies that effective policy is less about reacting to headline international price movements per se and more about weakening the domestic transmission mechanisms through which persistent price stress becomes entrenched undernourishment.

6.4. Policy implications

A policy reading of these results begins with a distinction between international prices as a *signal* and hunger outcomes as a *system response*. International food prices remain an important risk marker for SDG 2.1, yet the weak and intermittent statistically significant co-movement—once persistence is accounted for—cautions against mechanistic narratives in which global price stabilisation automatically delivers commensurate reductions in undernourishment. Policy effectiveness, therefore, turns on transmission channels and buffers: how world-price movements pass through to domestic prices and wages, how quickly purchasing power is protected, and whether nutrition-sensitive systems prevent adverse dietary substitution and longer-run scarring.

In practical terms, this shifts emphasis towards the institutions that protect real incomes during sustained inflation episodes. When food inflation compresses purchasing power, scalable cash transfers, school feeding, and child nutrition programmes can interrupt the pathway from price pressures to diet-quality deterioration, consistent with evidence linking food inflation to undernutrition outcomes [25]. The coherence results strengthen the case for treating international prices as an early-warning input rather than as a sufficient targeting rule: the same international movement can coincide with sharply different hunger trajectories depending on exchange-rate movements, domestic market integration, and the coverage and scalability of social protection.

Trade and market interventions require an equally careful interpretation. Some instruments can moderate domestic volatility in the short run; however, the literature cautions that widespread, uncoordinated interventions—particularly export restrictions and ad hoc controls—can externalise volatility and raise the global cost of stabilisation [9]. In a world of compound shocks, predictable policy frameworks, transparent information on stocks and trade measures, and credible rules for temporary interventions are likely to be more effective than discretionary responses that amplify uncertainty and disrupt private storage and trade incentives.

Finally, the SDG framing and the observed regime shift underscore that conflict and climate are not background correlates but structural determinants of both price surges and hunger incidence. The GRFC evidence that conflict remains a leading driver of acute food insecurity, interacting with economic shocks and climate extremes, strengthens the case for integrating early warning, humanitarian access and resilience investment into SDG 2 strategies [35]. Price monitoring should therefore sit alongside conflict-risk and climate-risk monitoring, with agreed triggers that activate scalable safety nets and nutrition responses when compound risks intensify. From an accountability perspective, the frequency mismatch between monthly price indices and annual, modelled PoU

© 2026 by the author(s). Distributed under a Creative Commons CC BY license.

Preprints.org (www.preprints.org) | NOT PEER-REVIEWED | Posted: 11 March 2026 doi:10.20944/preprints202603.0754.v1

suggests a division of labour: high-frequency price indicators are best positioned as early signals of stress, whereas PoU remains a lagging metric of structural progress. Evaluations should triangulate PoU with more responsive indicators (diet affordability, experience-based food insecurity measures, and acute malnutrition where available), rather than expecting PoU to validate short-run policy effects.

6.5. Limitations and Directions for Further Research

Several limitations are material for interpretation and should be stated prominently. First, the effective sample for the bivariate PoU–FPI coherence analysis is short (2001–2023; n = 23), which constrains inference at longer periodicities and makes edge effects and the cone of influence particularly consequential. As emphasised in the wavelet methods literature, finite samples can exaggerate apparent power and coherence at low frequencies, reinforcing the need for careful significance testing and restrained interpretation [10,29]. Importantly, however, the short sample does not render the coherence exercise uninformative: framed as a diagnostic against spurious dependence, the sharp gap between raw coherence and red-noise significance remains itself evidential and policy-relevant.

Second, PoU is a modelled indicator with non-trivial uncertainty bands; treating point estimates as observed values may understate uncertainty in the estimated association. This matters because the core finding concerns statistical significance after accounting for persistence: additional measurement uncertainty in PoU would, if anything, further caution against strong claims of tight global co-movement.

Third, global aggregation obscures the heterogeneity central to the welfare economics of food price changes. The international-to-domestic pass-through, the net buyer/seller composition of the poor, and the policy environment vary sharply across countries, implying that a global relationship can be weak even when country-level effects are meaningful [23]. This motivates extensions using panels or regional disaggregation to test whether coherence strengthens in import-dependent, conflict-affected, or highly urban contexts, and whether the post-2012 regime shift is concentrated in specific regions.

Fourth, the analysis is deliberately associational rather than causal. While phase patterns are informative diagnostics, they do not identify causal elasticities, particularly in the presence of common drivers and endogenous policy responses. Causal extensions would require credible exogenous variation in price shocks (e.g., weather-driven supply instruments, shipping disruptions, or policy discontinuities), or structural models linking prices, incomes and nutrition with transparent identifying assumptions [6,36].

Finally, the forecasting and scenario work inherits the instability documented in the historical relationship. Structural change—through climate acceleration, geopolitical fragmentation, or technological shifts—can render historical statistical mappings unreliable for extrapolation. This is precisely why scenario framing is defensible, but it should be presented as an invitation for iterative updating as new information emerges rather than as a definitive statement about 2030 outcomes [16].

7. Conclusions

This study contributes to sustainability-oriented food security research by re-examining whether international food price dynamics provide a reliable signal for global undernourishment trends and SDG 2.1 monitoring. The evidence supports a restrained, policy-relevant conclusion: the apparent food price–undernourishment relationship is unstable in aggregate and is easily overstated by approaches that do not adequately account for persistence and structural change.

Methodologically, the wavelet coherence framework—benchmarked against an autocorrelated red-noise null—shows that visually strong co-movement can largely reflect the internal autocorrelation of both series rather than robust dependence. Substantively, this implies that international price movements alone are an incomplete proxy for SDG 2.1 outcomes at the global level, and that headline correlations may be misleading in sustainability assessments that seek to infer

© 2026 by the author(s). Distributed under a Creative Commons CC BY license.

Preprints.org (www.preprints.org) | NOT PEER-REVIEWED | Posted: 11 March 2026 doi:10.20944/preprints202603.0754.v1

vulnerability or progress from global price indices. At the same time, the analysis does not imply that prices are irrelevant: where statistically defensible dependence is observed, it tends to concentrate at medium-run horizons, consistent with the design of PoU as a measure of habitual energy inadequacy and with the notion that undernourishment responds primarily to sustained affordability pressures rather than short-lived monthly volatility.

A second implication is that the price–undernourishment nexus is regime-dependent. The rolling correlation results indicate a shift in the association in the early 2010s, suggesting that the macro context shaping price transmission—through income dynamics, domestic market conditions, and exposure to compound shocks—has evolved. For sustainability and human development, this matters because it highlights the limits of constant-parameter representations and underscores the need for SDG monitoring frameworks that are robust to non-stationarity and structural breaks.

From a policy perspective, the findings motivate a shift from "price-centric" interpretations towards transmission-centric resilience. If global prices are an early signal rather than a sufficient predictor, then effective SDG 2.1 strategies should prioritise the domestic mechanisms that determine welfare incidence: protecting real purchasing power during sustained food inflation, scaling shock-responsive social protection and nutrition-sensitive programmes, strengthening market functioning and storage to reduce domestic amplification, and adopting credible, coordinated trade and emergency import arrangements that minimise destabilising spillovers. In sustainability terms, these measures support human capability by reducing the risk that temporary market stress translates into persistent losses in nutrition, health and developmental potential.

Finally, the scenario-based projections to 2030 should be interpreted as stress tests for SDG planning under deep uncertainty rather than as deterministic forecasts of hunger. The widening forecast uncertainty underscores that long-horizon outcomes are strongly conditioned by hard-to-predict disruptions (e.g., climate extremes, conflict escalation, and policy breaks). Accordingly, a prudent sustainability approach is to use scenarios to identify vulnerabilities and trigger points for anticipatory action, rather than to infer a single expected pathway to 2030.

Overall, the study's core sustainability contribution is twofold: (i) it provides a more conservative and statistically grounded diagnosis of when international food prices align with undernourishment dynamics, and (ii) it translates that diagnosis into policy-relevant guidance that emphasises resilience, equity and human development outcomes—consistent with the integrated nature of SDG progress.

Author Contributions: Conceptualization O.P., O.L., K.P., A.K., N.F., A.M., O.H. and T.V.; methodology O.P., O.L., K.P., A.K., N.F., A.M., O.H. and T.V.; software O.P., O.L., K.P., A.K., N.F., A.M., O.H. and T.V.; validation O.P., O.L., K.P., A.K., N.F., A.M., O.H. and T.V.; formal analysis O.P., O.L., K.P., A.K., N.F., A.M., O.H. and T.V.; investigation O.P., O.L., K.P., A.K., N.F., A.M., O.H. and T.V.; resources O.P., O.L., K.P., A.K., N.F., A.M., O.H. and T.V.; data curation O.P., O.L., K.P., A.K., N.F., A.M., O.H. and T.V.; writing—original draft preparation O.P., O.L., K.P., A.K., N.F., A.M., O.H. and T.V.; writing—review and editing O.P., O.L., K.P., A.K., N.F., A.M., O.H. and T.V.; visualization O.P., O.L., K.P., A.K., N.F., A.M., O.H. and T.V.; supervision O.P., O.L., K.P.; project administration O.P., O.L., K.P.; funding acquisition A.K., A.M., and T.V. All authors have read and agreed to the published version of the manuscript.

Funding: This work was supported by a subsidy from the Ministry of Education and Science for the AGH University of Kraków.

Institutional Review Board Statement: Not applicable.

Informed Consent Statement: Not applicable.

Data Availability Statement: The datasets analysed in this study are publicly available from the following sources: FAO Food Price Index (FPI): Monthly data (January 1990 to December 2025) are available from the Food and Agriculture Organisation of the United Nations at https://www.fao.org/worldfoodsituation/foodpricesindex/en/. Prevalence of Undernourishment (PoU): Annual data (2001–2023) are available from FAO's Food Security Indicators database at

© 2026 by the author(s). Distributed under a Creative Commons CC BY license.

Preprints.org (www.preprints.org) | NOT PEER-REVIEWED | Posted: 11 March 2026 doi:10.20944/preprints202603.0754.v1

https://www.fao.org/faostat/en/#data/FS. SDG Indicator 2.1.1: Official metadata and methodological documentation are available from the United Nations Statistics Division at https://unstats.un.org/sdgs/metadata/files/Metadata-02-01-01.pdf. FAO Commodity Sub-Indices: Monthly price indices for cereals, vegetable oils, meat, dairy, and sugar (1990–2025) are available from the same FAO Food Price Index database. All data were accessed in December 2025. The Python analysis code and processed datasets are available from the corresponding author upon reasonable request.

Conflicts of Interest: The authors declare no conflicts of interest.

Abbreviations

The following abbreviations are used in this manuscript:

Abbreviation	Definition
ADF	Augmented Dickey–Fuller (test)
AIC	Akaike Information Criterion
AR(1)	First-order autoregressive process
ARIMA	Autoregressive Integrated Moving Average
BIC	Bayesian Information Criterion
COI	Cone of Influence
CWT	Continuous Wavelet Transform
FAO	Food and Agriculture Organization of the United Nations
FPI	Food Price Index
GRFC	Global Report on Food Crises
IFAD	International Fund for Agricultural Development
LMICs	Low- and Middle-Income Countries
MAE	Mean Absolute Error
MSE	Mean Squared Error
OLS	Ordinary Least Squares
PACF	Partial Autocorrelation Function
PoU	Prevalence of Undernourishment
RF	Random Forest
RMSE	Root Mean Squared Error
SDG	Sustainable Development Goal
SDG 2.1	Sustainable Development Goal Target 2.1
UN	United Nations
UN DESA	United Nations Department of Economic and Social Affairs
UNSD	United Nations Statistics Division
UNICEF	United Nations Children's Fund
WFP	World Food Programme
WHO	World Health Organization

Appendix A

Table A1 presents the complete monthly forecast trajectory for the FAO Food Price Index from January 2026 to December 2030, generated using the hybrid ARIMA(1,1,1)-Random Forest model described in Section 4.3. Point forecasts represent the baseline scenario; 95% confidence intervals are derived from ARIMA prediction variance using a bootstrap (B = 1,000 iterations).

Table A1. Monthly FAO Food Price Index Forecasts (January 2026 – December 2030).

Month	Baseline	Lower 95% CI	Upper 95% CI
Jan 2026	123.2	105.4	141.0
Feb 2026	122.9	105.2	140.6
Mar 2026	122.7	105.0	140.4
Apr 2026	123.0	105.2	140.8
May 2026	123.5	105.6	141.4
Jun 2026	123.8	105.9	141.7
Jul 2026	124.0	106.0	142.0

© 2026 by the author(s). Distributed under a Creative Commons CC BY license.

Preprints.org (www.preprints.org) | NOT PEER-REVIEWED | Posted: 11 March 2026 doi:10.20944/preprints202603.0754.v1

Aug 2026	123.7	105.8	141.6
Sep 2026	123.4	105.6	141.2
Oct 2026	123.1	105.3	140.9
Nov 2026	122.8	105.1	140.5
Dec 2026	122.6	104.9	140.3
Jan 2027	123.1	86.7	159.4
Feb 2027	122.8	86.5	159.0
Mar 2027	122.6	86.3	158.8
Apr 2027	122.9	86.5	159.2
May 2027	123.4	86.9	159.8
Jun 2027	123.7	87.2	160.1
Jul 2027	123.9	87.3	160.4
Aug 2027	123.6	87.1	160.0
Sep 2027	123.3	86.9	159.6
Oct 2027	123.0	86.6	159.3
Nov 2027	122.7	86.4	158.9
Dec 2027	122.5	86.2	158.7
Jan 2028	123.1	74.9	171.2
Feb 2028	122.8	74.7	170.8
Mar 2028	122.6	74.5	170.6
Apr 2028	122.9	74.7	171.0
May 2028	123.4	75.1	171.6
Jun 2028	123.7	75.4	171.9
Jul 2028	123.9	75.5	172.2
Aug 2028	123.6	75.3	171.8
Sep 2028	123.3	75.1	171.4
Oct 2028	123.0	74.8	171.1
Nov 2028	122.7	74.6	170.7
Dec 2028	122.5	74.4	170.5
Jan 2029	123.1	65.5	180.6
Feb 2029	122.8	65.3	180.2
Mar 2029	122.6	65.1	180.0
Apr 2029	122.9	65.3	180.4
May 2029	123.4	65.7	181.0
Jun 2029	123.7	66.0	181.3
Jul 2029	123.9	66.1	181.6
Aug 2029	123.6	65.9	181.2
Sep 2029	123.3	65.7	180.8
Oct 2029	123.0	65.4	180.5
Nov 2029	122.7	65.2	180.1
Dec 2029	122.5	65.0	179.9
Jan 2030	123.1	57.5	188.6
Feb 2030	122.8	57.3	188.2
Mar 2030	122.6	57.1	188.0
Apr 2030	122.9	57.3	188.4
May 2030	123.4	57.7	189.0
Jun 2030	123.7	58.0	189.3
Jul 2030	123.9	58.1	189.6
Aug 2030	123.6	57.9	189.2
Sep 2030	123.3	57.7	188.8
Oct 2030	123.0	57.4	188.5
Nov 2030	122.7	57.2	188.1
Dec 2030	122.5	57.0	187.9

Note: All values expressed as index points (2014–2016 = 100). CI = confidence interval. Forecasts are recursive, with RF-predicted residuals feeding back as lagged inputs.

© 2026 by the author(s). Distributed under a Creative Commons CC BY license.

Preprints.org (www.preprints.org) | NOT PEER-REVIEWED | Posted: 11 March 2026 doi:10.20944/preprints202603.0754.v1

Appendix B

This appendix reports the results of unit root and stationarity tests used to determine the time series' order of integration and to inform model specification.

Appendix B.1. FAO Food Price Index (Monthly)

Table A2. Unit Root Tests for Monthly FPI (1990–2025).

Test	Statistic	p-value	Conclusion
ADF (levels, constant)	−1.65	0.457	Non-stationary
ADF (levels, constant + trend)	−2.31	0.428	Non-stationary
ADF (first difference)	−9.63	<0.001	Stationary
Phillips-Perron (levels)	−1.89	0.337	Non-stationary
Phillips-Perron (first difference)	−18.42	<0.001	Stationary
KPSS (levels, constant)	1.87	<0.01	Non-stationary
KPSS (first difference)	0.12	>0.10	Stationary

Note: ADF = Augmented Dickey-Fuller; KPSS = Kwiatkowski-Phillips-Schmidt-Shin. Lag selection by AIC (max 12). Critical values at 5% level.

Appendix B.2. Prevalence of Undernourishment (Annual)

Table A3. Unit Root Tests for Annual PoU (2001–2023).

Test	Statistic	p-value	Conclusion
ADF (levels, constant)	−1.42	0.571	Non-stationary
ADF (first difference)	−3.87	0.003	Stationary
KPSS (levels)	0.68	<0.05	Non-stationary

Note: Limited sample size (n = 23) reduces power of unit root tests. Results should be interpreted with caution.

Appendix B.3. Structural Break Tests

Table A4. Zivot-Andrews Structural Break Test Results.

Series	Break Date	t-statistic	5% CV	Result
FPI (intercept)	2007M09	−3.89	−4.80	No break
FPI (trend)	2006M11	−4.12	−4.42	No break
FPI (both)	2007M03	−4.67	−5.08	No break
PoU (intercept)	2014	−3.21	−4.80	No break

Note: CV = critical value. The Zivot-Andrews test endogenously determines the break date. Results suggest a unit root with no significant structural break in the stochastic trend.

Appendix C. Robustness Checks

Appendix C.1. Alternative Wavelet Specifications

We verified the robustness of wavelet coherence results to alternative methodological choices. Table A8 reports the proportion of statistically significant time-frequency cells under different Morlet wavelet central frequencies.

© 2026 by the author(s). Distributed under a Creative Commons CC BY license.

Preprints.org (www.preprints.org) | NOT PEER-REVIEWED | Posted: 11 March 2026 doi:10.20944/preprints202603.0754.v1

Table A5. Sensitivity to Wavelet Central Frequency.

Central frequency (ω_0)	% Significant cells	Mean coherence	Max coherence
5	7.2%	0.758	0.97
6 (baseline)	7.8%	0.765	0.97
7	8.4%	0.771	0.98

Note: Significance assessed at 95% level against AR(1) red-noise null (1,000 Monte Carlo simulations).

Appendix C.2. Alternative Null Models for Significance Testing

Table A6. Sensitivity to Null Model Specification.

Null model	% Significant cells	Interpretation
AR(1) (baseline)	7.8%	Sparse significance
AR(2)	8.1%	Consistent with baseline
ARFIMA(1,d,0)	6.9%	More conservative
White noise	34.2%	Overstates significance

Note: ARFIMA fractional integration parameter d estimated at 0.31 for FPI and 0.42 for PoU. White noise null included for comparison only—inappropriate for persistent series.

Appendix C.3. Forecast Model Comparison

Table A7 compares out-of-sample forecast performance across alternative model specifications using a rolling-origin evaluation framework (training window: 1990–2019; evaluation: 2020–2025).

Table A7. Out-of-Sample Forecast Performance Comparison.

Model	RMSE	MAE	MAPE (%)	Theil U
ARIMA(1,1,1)	8.42	6.87	5.91	0.89
ARIMA(2,1,2)	8.67	7.03	6.05	0.92
ETS(M,A,N)	9.31	7.68	6.62	0.98
Random Forest (standalone)	9.15	7.52	6.48	0.97
ARIMA(1,1,1)-RF Hybrid	7.89	6.34	5.46	0.84
Naïve (random walk)	9.47	7.81	6.73	1.00

Note: RMSE = root mean squared error; MAE = mean absolute error; MAPE = mean absolute percentage error; Theil U = Theil inequality coefficient (U < 1 indicates improvement over naïve forecast). Evaluation window: 72 months.

Appendix D. Sensitivity Analysis

Appendix D.1. Rolling Window Size Sensitivity

The rolling correlation analysis in Section 5.4 employs 5-year windows. Table A8 examines sensitivity to alternative window sizes.

Table A8. Regime Shift Detection Across Window Sizes.

Window size	Pre-2012 $\bar{r}$	Post-2012 $\bar{r}$	Shift magnitude	Transition year
3 years	−0.724	+0.583	1.307	2011–2012
5 years (baseline)	−0.791	+0.641	1.432	2011–2013
7 years	−0.812	+0.594	1.406	2012–2014

Note: $\bar{r}$ = mean Pearson correlation coefficient across windows in each regime. The regime shift is robust to the choice of window size.

© 2026 by the author(s). Distributed under a Creative Commons CC BY license.

Preprints.org (www.preprints.org) | NOT PEER-REVIEWED | Posted: 11 March 2026 doi:10.20944/preprints202603.0754.v1

Appendix D.2. Sub-Sample Analysis

Table A9 reports wavelet coherence statistics for distinct sub-periods to assess temporal stability.

Table A9. Sub-Sample Wavelet Coherence Analysis.

Sub-period	N (years)	Mean R^2	% Significant	Dominant phase
2001–2008 (pre-crisis)	8	0.71	5.2%	Anti-phase
2008–2015 (crisis/recovery)	8	0.78	9.1%	Transitional
2015–2023 (post-SDG)	9	0.82	11.3%	In-phase

Note: Sub-sample results should be interpreted cautiously due to reduced degrees of freedom. The increasing significance in later periods may reflect regime change rather than increased true coherence.

Appendix D.3. Leave-One-Year-Out Cross-Validation

Table A10 reports forecast accuracy metrics from leave-one-year-out cross-validation for the hybrid ARIMA-RF model.

Table A10. Leave-One-Year-Out Cross-Validation Results (2015–2025).

Year omitted	RMSE	MAE	MAPE (%)	Coverage (%)
2015	6.21	5.14	5.87	100
2016	5.87	4.92	5.52	100
2017	6.43	5.31	5.94	100
2018	7.12	5.89	6.21	100
2019	6.78	5.52	5.78	100
2020	9.34	7.81	7.42	92
2021	12.67	10.54	8.91	83
2022	18.42	15.23	11.87	75
2023	11.23	9.12	7.89	92
2024	8.56	7.01	6.34	100
2025	7.89	6.45	5.87	100
Mean	**9.14**	**7.54**	**7.06**	**95**

Note: Coverage = percentage of actual values falling within 95% confidence interval. Elevated errors in 2021–2022 reflect the unpredictable nature of the post-pandemic price surge.

Appendix E. Commodity Sub-Index Analysis

Appendix E.1. Correlation Structure Among Commodity Sub-Indices

Table A11 presents the pairwise Pearson correlation matrix for the five FAO commodity sub-indices over the full sample period (1990–2025).

Table A11. Correlation Matrix of FAO Commodity Sub-Indices (Monthly, 1990–2025).

	Cereals	Oils	Meat	Dairy	Sugar
Cereals	1.00	0.87	0.72	0.81	0.54
Vegetable Oils	0.87	1.00	0.68	0.79	0.61
Meat	0.72	0.68	1.00	0.74	0.41
Dairy	0.81	0.79	0.74	1.00	0.49
Sugar	0.54	0.61	0.41	0.49	1.00

Note: All correlations are significant at $p < 0.001$. Cereals and vegetable oils exhibit the strongest co-movement ($r = 0.87$), reflecting common drivers including energy costs and biofuel demand. Sugar shows the weakest correlation with other commodities.

© 2026 by the author(s). Distributed under a Creative Commons CC BY license.

Preprints.org (www.preprints.org) | NOT PEER-REVIEWED | Posted: 11 March 2026 doi:10.20944/preprints202603.0754.v1

Appendix E.2. Wavelet Coherence by Commodity Sub-Index

Table A12 reports wavelet coherence statistics between each commodity sub-index and global PoU, enabling identification of which commodity groups exhibit the strongest association with undernourishment.

Table A12. Wavelet Coherence Between Commodity Sub-Indices and Global PoU.

Commodity	Mean R^2	Max R^2	% Significant	Key scale (years)
Aggregate FPI	0.765	0.97	7.8%	3–5
Cereals	0.742	0.96	9.2%	3–5
Vegetable Oils	0.728	0.95	6.8%	4–6
Meat	0.681	0.92	5.1%	5–7
Dairy	0.712	0.94	6.3%	4–6
Sugar	0.623	0.89	4.7%	6–8

Note: Cereals exhibit the highest proportion of significant coherence cells (9.2%), consistent with their importance in caloric intake for food-insecure populations. Sugar shows the weakest coherence with PoU.

Appendix F. Technical Methodology Details

Appendix F.1. Continuous Wavelet Transform Specification

The continuous wavelet transform was computed using the Morlet mother wavelet:

$$\psi(\eta) = \pi^{(-1/4)} e^{(i\omega^0 \eta)} e^{(-\eta^2/2)}$$

where $\omega_0 = 6$ is the central frequency, providing optimal balance between time and frequency localisation. The wavelet scale s was sampled at fractional octaves with $\delta j = 0.125$, yielding 57 scales from 0.5 to 64 years.

Appendix F.2. Smoothing Operator for Coherence Estimation

Wavelet coherence requires smoothing in both time and scale to yield meaningful coherence estimates (without smoothing, coherence equals unity everywhere). Following Torrence and Compo (1998), we apply:

$$S(W) = S_{scale}\left(S_{time}(W_{xy})\right)$$

where S_{time} is a boxcar filter of width 0.6s (where s is the wavelet scale) and S_{scale} is a Gaussian filter of width 0.6 octaves.

Appendix F.3. Monte Carlo Significance Testing Procedure

Statistical significance was assessed using the following Monte Carlo procedure:

1. Estimate AR(1) coefficients for each series from the observed data
2. Generate 1,000 pairs of AR(1) surrogate series matching observed autocorrelation
3. Compute wavelet coherence for each surrogate pair
4. At each time-frequency location, determine the 95th percentile of surrogate coherence
5. Observed coherence exceeding this threshold is deemed statistically significant

This approach explicitly accounts for the tendency of persistent (red noise) processes to exhibit spurious coherence at low frequencies.

Appendix F.4. Hybrid ARIMA-RF Model Specification

The hybrid forecasting model combines linear and nonlinear components:

$$\widehat{y_{t+h}} = y_{t+h}^{\widehat{\text{ARIMA}}} + \varepsilon_{t+h}^{\widehat{\text{RF}}}.$$

© 2026 by the author(s). Distributed under a Creative Commons CC BY license.

Preprints.org (www.preprints.org) | NOT PEER-REVIEWED | Posted: 11 March 2026 doi:10.20944/preprints202603.0754.v1

ARIMA(1,1,1) specification: $\varphi_1 = 0.612$ (SE = 0.062), $\theta_1 = -0.158$ (SE = 0.076)

Random Forest hyperparameters: n_estimators = 100, max_depth = 10, min_samples_split = 5, min_samples_leaf = 2, n_lags = 5. Cross-validation performance: $R^2 = 0.52 \pm 0.08$; MAE = 3.2 ± 0.7 index points.

Bootstrap confidence intervals (B = 1,000) account for both parameter uncertainty and residual variability.

Appendix F.5. Software and Reproducibility

All analyses were conducted in Python 3.12 using:

- pywt 1.5.0 – Continuous wavelet transform computation
- statsmodels 0.14.1 – ARIMA estimation and diagnostics
- scikit-learn 1.4.0 – Random Forest implementation
- numpy 1.26.3 – Numerical computations
- scipy 1.12.0 – Statistical tests

Random seed fixed at 42 for all stochastic procedures. Analysis code available upon request.

Appendix G

Figure A1 displays the continuous-wavelet power spectrum of the annual prevalence of undernourishment series. The spectrum reveals dominant power at periodicities of 4–6 years, with elevated variance during 2008–2012 (food crisis period) and 2020–2023 (pandemic and post-pandemic period). The cone of influence excludes approximately 40% of the time-frequency plane due to the short sample length.

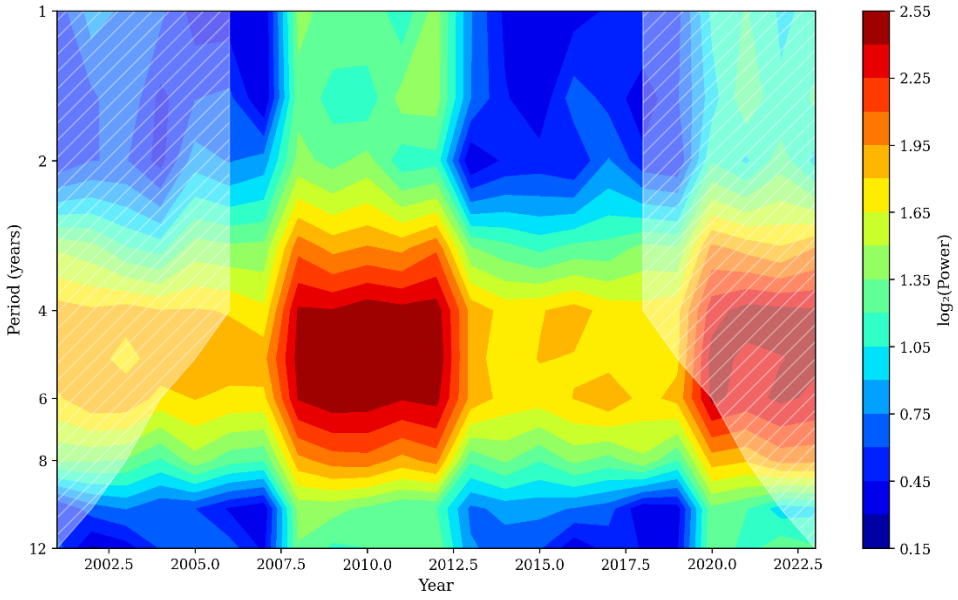

Figure A1. Wavelet Power Spectrum of Global PoU (2001–2023).

Figure A2 presents the cross-wavelet transform, which identifies regions of high common power between the series prior to normalisation. Unlike coherence, cross-wavelet power can be dominated by either series. The figure reveals pronounced common power in the 3–5 year band during 2006–2012, coinciding with the global food price crisis.

Figure A3 displays rose diagrams of phase angles for significant coherence cells, stratified by period band (1–2, 2–4, 4–8, 8+ years). At medium frequencies (3–5 years), phase angles cluster around −135° to −150°, indicating that PoU leads FPI by approximately 1.1–1.4 years. This counterintuitive finding is discussed in Section 6.1.

© 2026 by the author(s). Distributed under a Creative Commons CC BY license.

Preprints.org (www.preprints.org) | NOT PEER-REVIEWED | Posted: 11 March 2026 doi:10.20944/preprints202603.0754.v1

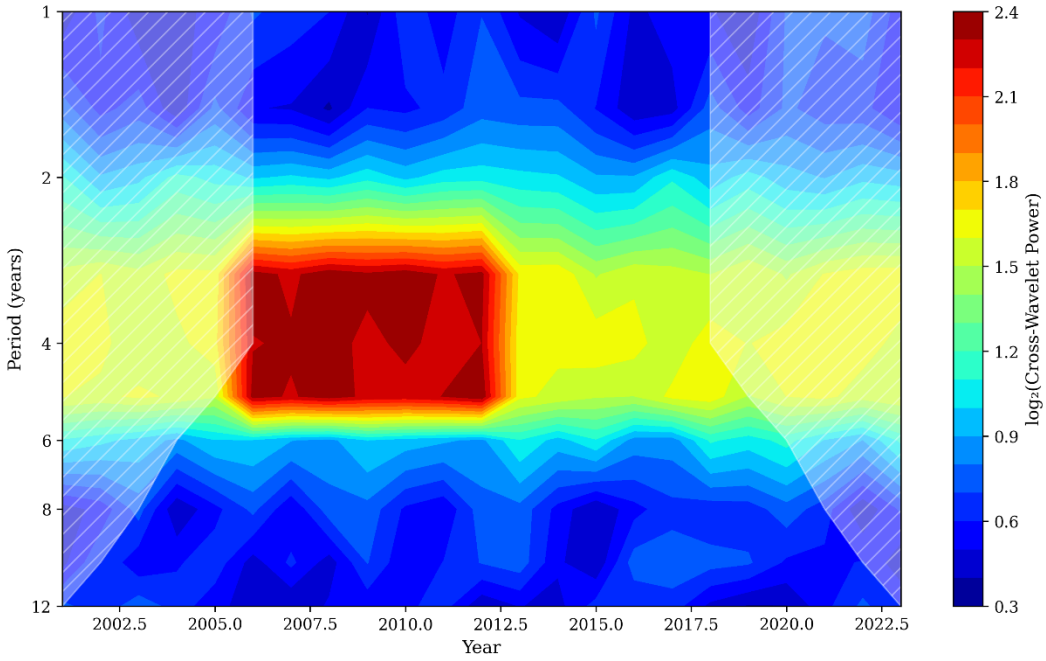

Figure A2. Cross-Wavelet Transform (FPI × PoU).

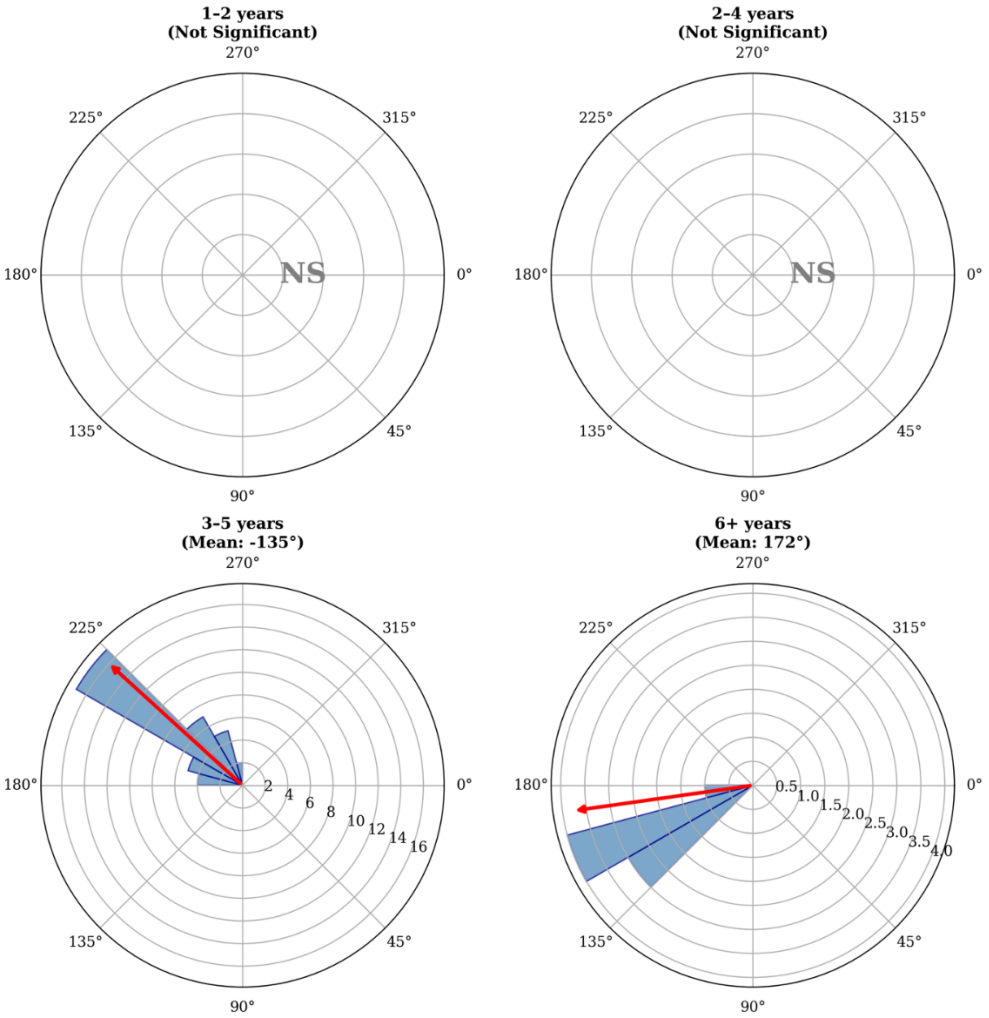

Figure A3. Phase Angle Distribution by Period Band.

© 2026 by the author(s). Distributed under a Creative Commons CC BY license.

Preprints.org (www.preprints.org) | NOT PEER-REVIEWED | Posted: 11 March 2026 doi:10.20944/preprints202603.0754.v1

Figure A4 presents autocorrelation function (ACF) and partial autocorrelation function (PACF) plots for: (a) raw monthly FPI, (b) first-differenced FPI, (c) ARIMA(1,1,1) residuals, and (d) hybrid model residuals. The slow decay of ACF in panel (a) confirms non-stationarity. Panel (d) shows residuals consistent with white noise, validating the hybrid model specification.

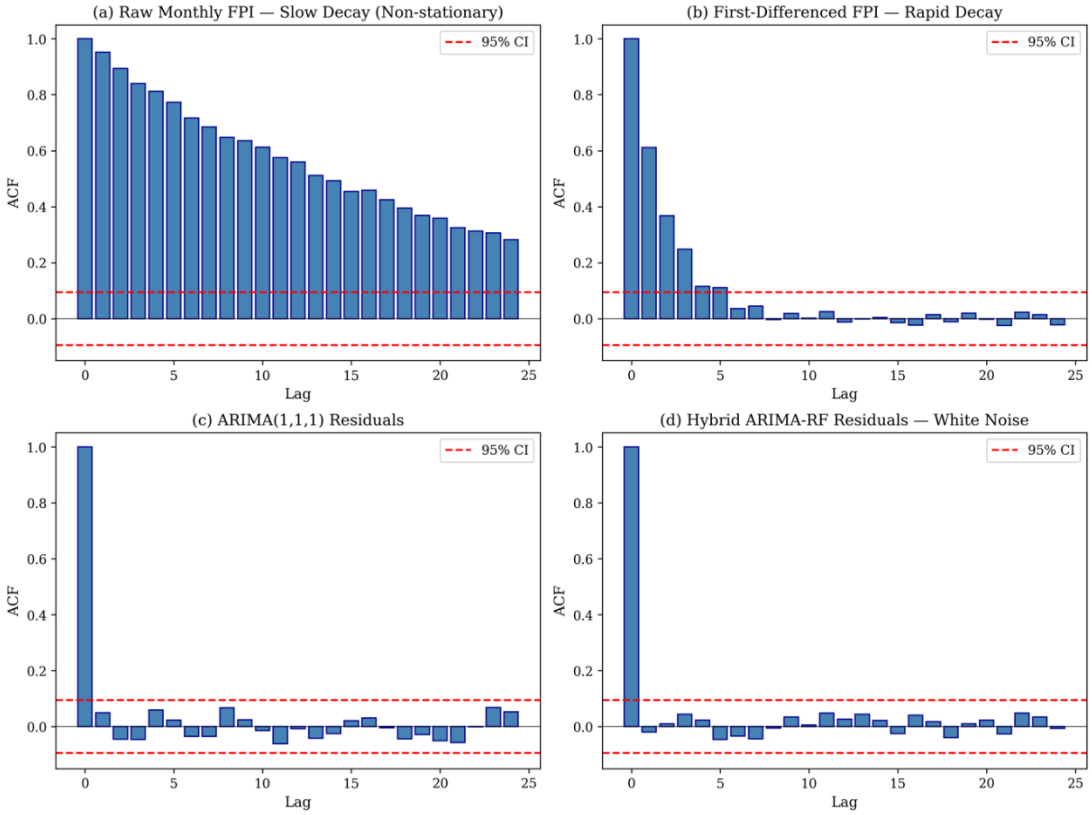

Figure A4. ACF and PACF Diagnostics.

Figure A5 presents a fan chart showing the complete forecast distribution for 2026-2030. The fan includes 50%, 80%, and 95% prediction intervals, illustrating the rapid expansion of uncertainty over the forecast horizon. By 2030, the 95% interval spans 131 index points (57.5 to 188.6).

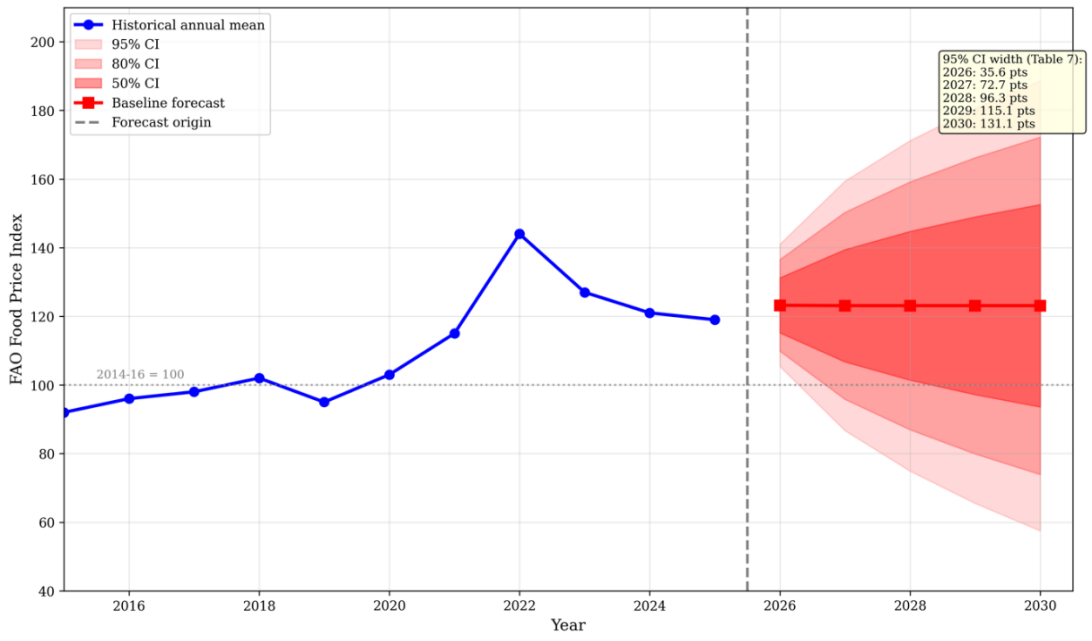

© 2026 by the author(s). Distributed under a Creative Commons CC BY license.

Preprints.org (www.preprints.org) | NOT PEER-REVIEWED | Posted: 11 March 2026 doi:10.20944/preprints202603.0754.v1

Figure A5. Forecast Fan Chart (2026–2030).

Figure A6 presents a 2×3 panel of wavelet coherence plots for each commodity sub-index (cereals, vegetable oils, meat, dairy, sugar) and for global PoU and the aggregate FPI. Cereals exhibit the largest region of significant coherence at 3–5-year periodicities, consistent with their caloric importance to food-insecure populations.

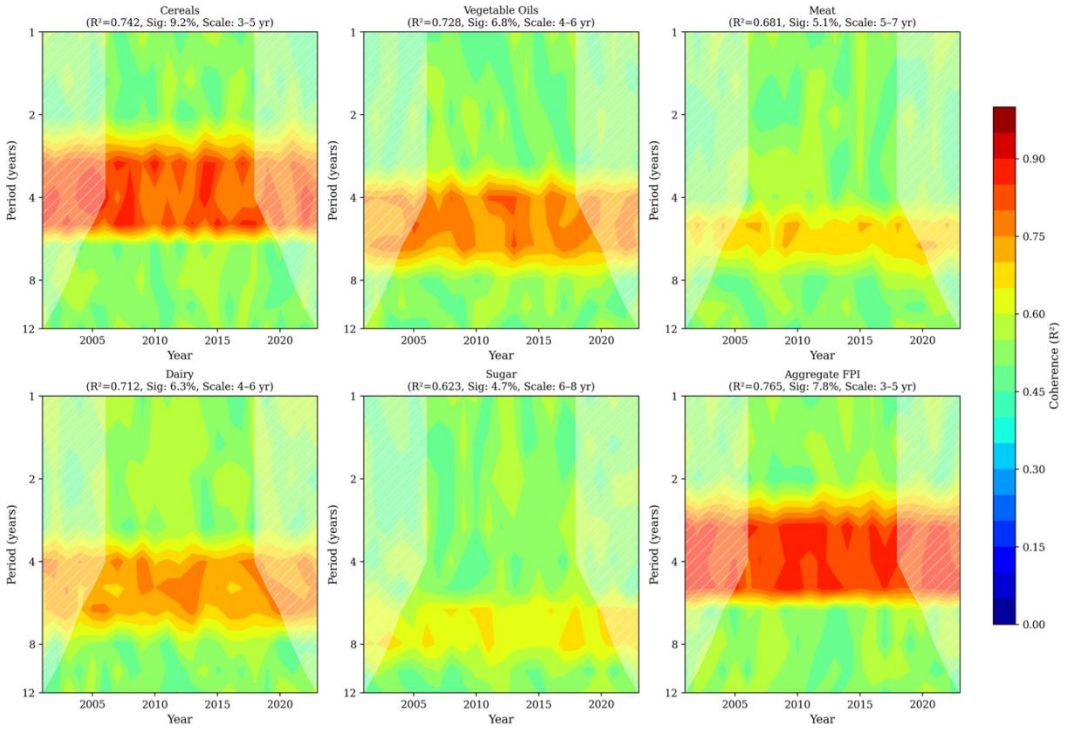

Figure A6. Commodity Sub-Index Wavelet Coherence Panels.

References

1. UN DESA. Goal 2: End Hunger, Achieve Food Security and Improved Nutrition and Promote Sustainable Agriculture. Available online: https://sdgs.un.org/goals/goal2 (accessed on 28 January 2026).
2. World Bank. Commodity Markets Outlook, January **2025**; World Bank: Washington, DC, USA, 2025. Available online: https://openknowledge.worldbank.org/handle/10986/41639 (accessed on 28 January 2026).
3. World Bank. Commodity Markets Outlook, April 2025; World Bank: Washington, DC, USA, 2025. Available online: https://openknowledge.worldbank.org/bitstreams/e19a3aa1-e28a-480c-a641-a61469989395/download (accessed on 28 January 2026).
4. World Bank. Food Security Update 120 (19 December 2025); World Bank: Washington, DC, USA, 2025. Available online: https://thedocs.worldbank.org/en/doc/40ebbf38f5a6b68bfc11e5273e1405d4-0090012022/related/Food-Security-Update-120-December-19-2025.pdf (accessed on 28 January 2026).
5. Wright, B.D. The Economics of Grain Price Volatility. *Appl. Econ. Perspect. Policy* **2011**, 33, 32–58. https://doi.org/10.1093/aepp/ppq033
6. Wright, B.D. Global Biofuels: Key to the Puzzle of Grain Market Behaviour. *J. Econ. Perspect.* **2014**, 28, 73–98. https://doi.org/10.1257/jep.28.1.73
7. UNSD. Metadata for SDG Indicator 2.1.1: Prevalence of Undernourishment; United Nations Statistics Division: New York, NY, USA, 2023. Available online: https://unstats.un.org/sdgs/metadata/files/Metadata-02-01-01.pdf (accessed on 28 January 2026).
8. FAO. Rome Declaration on World Food Security and World Food Summit Plan of Action; FAO: Rome, Italy, 1996.

© 2026 by the author(s). Distributed under a Creative Commons CC BY license.

Preprints.org (www.preprints.org) | NOT PEER-REVIEWED | Posted: 11 March 2026 doi:10.20944/preprints202603.0754.v1

9. Pieters, H.; Swinnen, J. Trading-Off Volatility and Distortions? Food Policy during Price Spikes. *Food Policy* 2016, 61, 27–39. https://doi.org/10.1016/j.foodpol.2016.01.004
10. Torrence, C.; Compo, G.P. A Practical Guide to Wavelet Analysis. Bull. Am. Meteorol. Soc. **1998**, 79, 61–78. https://doi.org/10.1175/1520-0477(1998)079<0061:APGTWA>2.0.CO;2
11. Grinsted, A.; Moore, J.C.; Jevrejeva, S. Application of the Cross Wavelet Transform and Wavelet Coherence to Geophysical Time Series. Nonlinear Process. Geophys. **2004**, 11, 561–566. https://doi.org/10.5194/npg-11-561-2004
12. Pérez-Escamilla, R.; Cunningham, K.; Moran, V.H. Food Security and the 2015–2030 Sustainable Development Goals: From Human to Planetary Health. Curr. Dev. Nutr. **2018**, 2, nzy024. https://doi.org/10.1093/cdn/nzy024
13. Gani, A.; Prasad, B.C. Food Security and Human Development. Int. J. Soc. Econ. **2007**, 34, 310–319. https://doi.org/10.1108/03068290710741570
14. FAO. The FAO Food Price Index: Technical Background. Food Outlook, June 2020; FAO: Rome, Italy, 2020.
15. FAO. FAO Food Price Index. Available online: https://www.fao.org/worldfoodsituation/foodpricesindex/en/ (accessed on 28 January 2026).
16. FAO; IFAD; UNICEF; WFP; WHO. The State of Food Security and Nutrition in the World 2025 (SOFI 2025); FAO: Rome, Italy, 2025. Available online: https://data.unicef.org/resources/sofi-2025 (accessed on 28 January 2026).
17. FAO; IFAD; UNICEF; WFP; WHO. The State of Food Security and Nutrition in the World 2024—Financing to End Hunger, Food Insecurity and Malnutrition in All Its Forms; FAO: Rome, Italy, 2024. https://doi.org/10.4060/cd1254en
18. FAO; IFAD; UNICEF; WFP; WHO. The State of Food Security and Nutrition in the World 2025—Addressing High Food Price Inflation for Food Security and Nutrition; FAO: Rome, Italy, 2025. https://doi.org/10.4060/cd6008en
19. FSIN; GNAFC. Global Report on Food Crises 2025; Food Security Information Network: Rome, Italy, 2025. Available online: https://www.fightfoodcrises.net/grfc-2025 (accessed on 28 January 2026).
20. von Grebmer, K.; Bernstein, J.; Mukerji, R.; Patterson, F.; Wiemers, M.; Ni Cheilleachair, R.; et al. 2025 Global Hunger Index: Hunger and Conflict in an Uncertain World; Welthungerhilfe: Bonn, Germany; Concern Worldwide: Dublin, Ireland, 2025. Available online: https://www.globalhungerindex.org (accessed on 28 January 2026).
21. Abbott, P.; Hurt, C.; Tyner, W. What's Driving Food Prices in 2011? Farm Foundation Issue Report; Farm Foundation: Oak Brook, IL, USA, 2011. Available online: https://www1.eere.energy.gov/bioenergy/pdfs/farm_foundation_whats_driving_food_prices.pdf (accessed on 28 January 2026).
22. Gilbert, C.L. How to Understand High Food Prices. J. Agric. Econ. **2010**, 61, 398–425. https://doi.org/10.1111/j.1477-9552.2010.00248.x
23. Ivanic, M.; Martin, W. Implications of Higher Global Food Prices for Poverty in Low-Income Countries. Agric. Econ. **2008**, 39, 405–416. https://doi.org/10.1111/j.1574-0862.2008.00347.x
24. Cook, J.T.; Frank, D.A. Food Security, Poverty, and Human Development in the United States. Ann. N. Y. Acad. Sci. **2008**, 1136, 193–209. https://doi.org/10.1196/annals.1425.001
25. Headey, D.; Ruel, M. Food Inflation and Child Undernutrition in Low and Middle-Income Countries. Nat. Commun. **2023**, 14, 5761. https://doi.org/10.1038/s41467-023-41543-9
26. Aguiar-Conraria, L.; Soares, M.J. The Continuous Wavelet Transform: Moving beyond Uni- and Bivariate Analysis. J. Econ. Surv. **2014**, 28, 344–375. https://doi.org/10.1111/joes.12012
27. Pal, D.; Mitra, S.K. Time-Frequency Contained Co-Movement of Crude Oil and World Food Prices: A Wavelet-Based Analysis. Energy Econ. **2017**, 62, 230–239. https://doi.org/10.1016/j.eneco.2016.12.020
28. Mastroeni, L.; Mazzoccoli, A.; Quaresima, G.; Vellucci, P. Wavelet Analysis and Energy-Based Measures for the Oil-Food Price Relationship as a Footprint of Financialisation Effect. Resour. Policy **2022**, 77, 102692. https://doi.org/10.1016/j.resourpol.2022.102692
29. Maraun, D.; Kurths, J. Cross Wavelet Analysis: Significance Testing and Pitfalls. Nonlinear Process. Geophys. **2004**, 11, 505–514. https://doi.org/10.5194/npg-11-505-2004

© 2026 by the author(s). Distributed under a Creative Commons CC BY license.

Preprints.org (www.preprints.org) | NOT PEER-REVIEWED | Posted: 11 March 2026 doi:10.20944/preprints202603.0754.v1

30. Li, X.; Zhang, Y.; Wang, H. Agricultural Product Price Forecasting Methods: A Review. Agriculture **2023**, 13, 1671. https://doi.org/10.3390/agriculture13091671
31. Jadhav, V.; Chinnappa Reddy, B.V.; Gaddi, G.M. Application of the ARIMA Model for Forecasting Agricultural Prices. J. Agric. Sci. Technol. **2017**, 19, 981–992. Available at: http://ir.jkuat.ac.ke/bitstream/handle/123456789/3583/JAST_Volume%2019_Issue%205_Pages%20981-992.pdf (accessed on 28 January 2026).
32. Manogna, R.L.; Dharmaji, V.; Sarang, S. Enhancing Agricultural Commodity Price Forecasting with Deep Learning. Sci. Rep. **2025**, 15, 20903. https://doi.org/10.1038/s41598-025-05103-z
33. Sari, M.; Duran, S.; Kutlu, H.; Guloglu, B.; Atik, H. Various Optimised Machine Learning Techniques to Predict Agricultural Commodity Prices. Neural Comput. Appl. **2024**, 36, 11439–11459. https://doi.org/10.1007/s00521-024-09679-x
34. Paul, R.K.; Yeasin, M.; Kumar, P.; Kumar, P.; Balasubramanian, M.; Roy, H.S.; Paul, A.K.; Gupta, A. An ARIMA-LSTM Model for Predicting Volatile Agricultural Price Series with Random Forest Technique. Appl. Soft Comput. **2023**, 149, 110958. https://doi.org/10.1016/j.asoc.2023.110958
35. GRFC. Global Report on Food Crises 2025; Food Security Information Network (FSIN): Rome, Italy, 2025. Available online: https://www.fightfoodcrises.net/report/global-report-food-crises-2025/ (accessed on 28 January 2026).
36. Mitchell, D. A Note on Rising Food Prices; World Bank Policy Research Working Paper 4682; World Bank: Washington, DC, USA, 2008. Available online: https://documents1.worldbank.org/curated/en/229961468140943023/pdf/WP4682.pdf (accessed on 28 January 2026).
37. Torrence, C.; Webster, P.J. Interdecadal Changes in the ENSO-Monsoon System. J. Clim. **1999**, 12, 2679–2690. https://doi.org/10.1175/1520-0442(1999)012<2679:ICITEM>2.0.CO;2

Disclaimer/Publisher's Note: The statements, opinions and data contained in all publications are solely those of the individual author(s) and contributor(s) and not of MDPI and/or the editor(s). MDPI and/or the editor(s) disclaim responsibility for any injury to people or property resulting from any ideas, methods, instructions or products referred to in the content.

© 2026 by the author(s). Distributed under a Creative Commons CC BY license.